Journal of Global Optimization (2025) 91:95–127
https://doi.org/10.1007/s10898-024-01439-4

Nested benders decomposition for a deterministic biomass feedstock logistics problem

Sanchit Singh[1] · **Subhash C. Sarin**[1] · **Sandeep Singh Sangha**[1]

Received: 11 May 2023 / Accepted: 2 October 2024 / Published online: 9 November 2024

Abstract

In this paper, we address a biomass feedstock logistics problem to supply biomass from production fields to satellite storage locations (SSLs) and from there to bioenergy plants (BePs) and then to a biorefinery. It entails a new problem feature of routing load-out equipment sets among the SSLs to perform loading/unloading of biomass and/or its pre-processing operations. The ownership of the loading equipment is a very capital-intensive link of the ethanol production supply chain, which when loaded onto trucks and routed along the logistics chain significantly brings down the ethanol production costs. This will make ethanol a cost-competitive alternative to fossil fuels, lead to sustainable use of fossil fuels and add to the overall relevance of the bioenergy sector. In this regard, the objective of our problem is to minimize the total cost incurred due to the ownership of equipment sets, fixed setups, and land rental cost, as well as the cost of transporting biomass from the fields to the BePs and biocrude oil from the BePs to the refinery. A mixed-integer mathematical model of the problem is presented, and a nested Benders decomposition-based solution approach is developed which involves decomposing this large problem into three stages. Stage 1 deals with the selection of fields, BePs, and SSLs, and assignment of fields to the SSLs. The remaining model consists of multiple Capacitated Vehicle Routing Problems (CVRPs) that are separable over individual BePs. For each BeP, the CVRP is further decomposed into Stage 2 and Stage 3 sub-problems where the Stage 2 problem is an allocation problem that assigns SSLs to tours associated to each BeP, and the Stage 3 problem is a variant of Traveling Salesman Problem (TSP) that determines the sequence in which equipment is routed over the predesignated set of SSLs for each tour. These sub-problems are integer programs rather than linear programs. First novelty of our proposed approach is to effectively handle the integrality of variables arising due to the consideration of the routing of load-out equipment. Second is solution methodology and in the use of proposed multi-cut version of optimality cuts that capture the solution value at an integer solution for the sub-problems. These cuts aid in faster convergence and are shown to be stronger than those proposed in the literature. The applicability of the proposed methodology is demonstrated by applying it to a real-life problem that utilizes available GIS data for the catchment area of regions around Gretna and Bedford in Virginia. We then solved a set of varying problem size instances using the state-of-the-art CPLEX® Branch-and-Bound and Benders Strategy methods. The CPLEX® algorithms struggled to solve instances even 10 times smaller than the real-life problem size instances; with MIP optimality gaps ranging from 5.85% to 82.79% in the allowed time limit of 10,000 s. On the other hand, our proposed nested Benders decomposition algorithm

Extended author information available on the last page of the article

was able to achieve faster convergence and provided optimal solutions for all the considered problem instances with an average CPU run-time of around 3,700 s. This validates the efficacy and superiority of our solution approach. Lastly, we summarize our work and point out some interesting potential future research opportunities.

Keywords Scheduling · Logistics · Optimization · Mathematical modeling · Biofuels

1 Introduction and motivation

Biofuel is a liquid fuel that is used primarily for transportation. Besides biodiesel (a fuel that is typically made from soybean, canola, or other vegetable oils), ethanol is another important category of biofuel that can produced from sources like corn [61], sugarcane [39], and other forest-based products [21] and [40]. Most of the ethanol produced in the U.S. is distilled from corn kernels. Contemporary research indicates that this process not only results in higher food prices but also is insufficient in meeting the desired production goals. This has given rise to the second generation of biofuel to be produced from the cellulosic feedstock (switchgrass) that is available in different geographic regions. Recently, there has been a significant increase in interest and active government endeavors to support the efforts towards the use of sustainable energy resources. Amidst rising concerns over the use of fossil fuels because of their impact on global climate change, and to reduce dependence on petroleum, the U.S. Congress adopted a Renewable Fuel Standard (RFS) in 2005 and expanded it under the Energy Independence and Security Act (EISA), 2007, with the focus on increasing production of advanced biofuels. Among its many guidelines and directives, this legislative act specifies domestic production targets on advanced biofuels to be 21.0 billion gallons by 2022, of which 16.0 billion gallons must be produced in the form of cellulosic biofuel. Since the target was not met by 2022, the U.S. Environmental Protection Agency (EPA) took a firm stance and published the 'Set Rule' in July 2023. According to this rule, the total renewable fuel volume requirements must increase from 1.5% to 8.2% over the next three years (2023 to 2025). Furthermore, as we confront the challenge of depleting fossil fuel reserves, investing in cellulosic biofuel production is imperative. Unlike traditional biofuels like corn ethanol, cellulosic biofuels offer a more sustainable solution by utilizing non-food biomass sources such as agricultural residues, grasses, and wood chips. The production of cellulosic biofuels not only reduces greenhouse gas emissions but also addresses concerns about food-versus-fuel competition. Therefore, it is essential to accelerate research and development efforts in cellulosic biofuel production to overcome existing economic challenges and scale up production. On a global scale, there has been a significant drive to increase awareness regarding cellulosic biofuel production, alongside a call for robust policy backing and investment in the necessary infrastructure. In Europe, policy support for cellulosic biofuel production in the UK dates back to the mid-2000s, with initiatives such as the Renewable Transport Fuel Obligation (RTFO) and the establishment of grant schemes. The commercial-scale operation of INEOS Bio's biorefinery in 2012 marked a significant milestone in the country's commitment to cellulosic biofuel production. Similarly, in Germany, government-backed Clariant Sunliquid operates a plant that converts agricultural residues into cellulosic ethanol using innovative enzymatic conversion processes. In Asia, both India and China intensified their focus on cellulosic biofuels since the late 2000s and early 2010s. India introduced the National Policy on Biofuels in 2009, while China implemented various policy measures to support research and production, leading to the establishment of several bioenergy plants and

refineries. In the Australasia region, Australia and New Zealand have seen increased policy support since the 2010s. Australia's initiatives include funding programs by the Australian Renewable Energy Agency (ARENA) and biofuel mandates in some states. Similarly, New Zealand has invested in research and development alongside industry partnerships to overcome technological challenges and establish sustainable biomass supply chains. Our research efforts are aligned with these initiatives and to support companies in the bioenergy sector that are investing in cellulosic biofuel production facilities and contributing towards reaching the total renewable fuel volume targets. For more insights into the recent global efforts related to cellulosic biofuel production, ongoing research review, policy support, and the establishment of bioenergy plants and refineries, we direct the reader to [7, 24, 43, 50, 78], and [79]. In conclusion, compelling evidence suggests that the demand for this renewable fuel source will become increasingly essential in the near future. Therefore, it is crucial that we proactively prepare for this forthcoming opportunity.

In this regard, our aim in this paper is to show that production of ethanol from a seasonal switchgrass (as an advanced biofuel alternative) can be an economically viable (cost-competitive in comparison to fossil fuels) option in the USA contrary to the current view of it being significantly costlier than the fossil fuels. We do this by minimizing the overall biomass feedstock logistics cost. This paper addresses a large-scale biomass feedstock logistics problem that involves supplying biomass from production fields to satellite storage locations (SSLs), from there to bioenergy plants (BePs), and then to a biorefinery. To effectively handle and solve this large problem, we developed a nested Benders decomposition solution approach that decomposes the problem into multiple stages (sub-problems and sub-subproblems) to effectively handle the decisions. With the focus on improving its convergence, we also developed a novel set of optimality cuts that are stronger than those presented in the literature. In the next sections, we first present a brief background related to the problem of interest and then state the problem in detail. Subsequently, a thorough discussion on relevant work from the literature is presented along with some research gaps and highlights of our contributions.

1.1 Background and problem statement

A biomass feedstock logistics problem that we address belongs to the production of ethanol from a seasonal harvest of switchgrass (a cellulosic feedstock). The biomass is hauled from production fields to satellite storage locations (SSLs), which serve as intermediate storage places. It is loaded on the racks/trailers by a specialized equipment system at an SSL and subsequently carried to a bioenergy plant (BeP) by delivery trucks. At a BeP, the cellulosic content in the biomass is converted into bio-crude oil. This bio-crude oil is then transported from a BeP to a refinery for final conversion and use as an energy product such as fuel ethanol.

The cost incurred for transporting biomass from production fields until its conversion to an energy product at a refinery is known to constitute a large portion of the cost of biofuel production. Fales et al. [35] report that this transportation cost amounts to 35–60% of the total cost of ethanol biofuel incurred over its entire supply chain. Raw biomass not only has a relatively low haul density, but also, the equipment designed for hauling biomass in the field is inefficient on the roadways compared with the use of tractor-trailer trucks. It is for this purpose that we employ satellite storage locations (SSLs), distributed throughout the production region for storing biomass hauled from production fields. Several previous studies have used intermediate locations in between the fields and a BeP for storing biomass, and they have attested to their effectiveness. Morey et al. [60] and Zhu et al. [92] call these

facilities "local storages" and "warehouses", respectively. Cundiff et al. [26] and Lamers et. al. [46] define an SSL to be a dedicated uncovered gravel piece of land within a field that is close to highways or secondary roads. A specialized mobile equipment system is used to load/unload biomass at SSLs and/or to perform pre-processing operations, like densification. We also permit the equipment system to move from its current SSL location to the next once a requisite amount of biomass has been shipped from that location since keeping such equipment fixed at all the sites will result in excessive costs [43] because of acquisition of a larger number of equipment sets. The addition of this feature to the problem is challenging as it complicates the problem formulation and demands effective handling. With this background, we now state the problem as follows:

Problem Statement: *The Deterministic Biomass Feedstock Logistics Problem (BLP) that we address in this paper can be stated as follows: For a given set of production fields and potential SSL locations, design an optimal logistics network consisting of production fields and SSLs, together with an assignment of production fields to their respective SSLs, locations of the BePs from a set of predetermined candidate locations and the allocation of SSLs to the BePs, to minimize the total cost on an annual basis incurred for transporting (1) biomass from each chosen production field to its corresponding SSL, (2) biomass from each chosen SSL to a BeP, (3) bio-crude oil from each BeP to the refinery, and (4) for routing the mobile equipment system(s) among the SSLs.* In practice, an end-to-end biomass logistics system would involve a single refinery being fed by multiple BePs situated at locations where the biomass is in abundance. For reasons that the BePs do not compete with each other for minimum fixed biomass intake, they are kept widespread. As such, all BeP candidate locations operate with mutually exclusive clusters of farms, SSLs, and mobile equipment systems.

The main novelty of this paper is in developing an algorithm to effectively handle the integrality of variables arising because of the consideration of the routing of load-out equipment, a feature that is complicating and that has not been addressed in the literature. Ownership of loading equipment is very capital-intensive link of the ethanol production supply chain which if loaded on the trucks and routed along will bring down the production costs of ethanol significantly. For this reason, we consider a deterministic version of the problem. Once a method for the solution of this problem is established, it would aid in addressing other relevant features like stochasticity in demand as well as biomass yield, biomass quality, and equipment availability.

2 Literature review

In this section, we first give a brief overview of the work on biomass feedstock supply chain design problems and its different variants. The review comprises of the relevant model formulations and approaches, the advancements in tackling different features involved with similar problems, the adopted solution methodologies in the literature, and the research gaps. Then a brief outline of the paper and the contributions of our work are provided.

The idea of production of ethanol from seasonal switchgrass and using it as an alternative to fossil fuels has now been around for nearly two decades. There are many challenges and trade-offs associated with the biomass supply chains which are concisely categorized into technical, economical/financial, social, environmental, policy and regulatory in [52] and [60]. But the main limiting factor that still persists is its high total cost of production. The economic viability of ethanol has been extensively studied in the literature (see [7, 21, 24, 26]). [7]

enumerates and assesses different cost estimates and technical factors associated with the supply chain and production of ethanol from switchgrass. Some of the main costs associated with such biomass supply chains are biomass purchase costs, transportation costs, biomass storage facility costs, loading/unloading equipment cost, pre-processing and refinery costs, etc. among others. It also provides a good estimate of biofuel demand and the abundance of switchgrass availability in different regions of Unites States. Biofuel supply chain design has been studied extensively with emphasis on a variety of features. Supply chain design under competitive agricultural land use and market equilibrium constraints is studied by [13, 14], and [15]. [12] addressed the biofuel supply chain planning under traffic congestion. Renewable supply chains integrated with district heating systems are presented by [17]. Biofuel life-cycle studies have been conducted in [21, 69, 84], and [85]. Biomass supply chain design optimization studies that focus on facility location, delivery systems, logistics, and capacity planning are presented in [24, 26–28, 36, 46], and [93]. Sustainability and GIS-based spatial issues are some of the other features that have also been considered in biomass supply chain design. We direct the readers to [7, 9, 14, 53, 63, 67, 71, 72, 83, 89], and [91] for a review of problems on the former, while for the latter, see [34, 41, 49, 70, 87], and [92]. Biomass supply chain design problem under different risks is addressed in [11] and [13]. Another prominent feature that affects the biomass supply chain is its quality variability across regions due to factors like weather, climate, terrain, etc. (see [1] and [22]). Such aspects are beyond the scope of this paper as they will lead to entirely different problems. However, our problem can be easily extended to include some if not all of the above features as additional constraints. As indicated in the name of the problem itself (biomass feedstock logistics), the focus of our research is to optimize the logistics involved in the biomass feedstock supply chain. For some interesting non-mathematical biomass supply chain optimization approaches we direct the reader to [5, 6, 29, 30, 33], and [77]. [31] uses a simulation technique to optimize the logistics of a biofuel collection problem. The authors develop an interesting game theory-based approach to handle the decisions related to agricultural land use and market equilibrium in [14]. We handle the problem by formulating it as a mixed-integer mathematical programming model.

A variety of different modelling constructs have been employed in the literature to formulate the biomass supply chain problems. Although there is quite a bit of overlap, we broadly categorize the relevant modeling approaches from literature into linear programming, mixed-integer linear programming, mathematical programming under uncertainty, and multi-objective mathematical programming. Some key references from these categories are presented in Table 1. Since, all the features of the problem considered in this paper are taken as deterministic, therefore, the stochastic and robust approaches are not applicable to our problem. For the convenience of the reader, we list some relevant studies from literature: for stochastic modeling of biomass supply chains, see [2, 10, 38, 51, 56, 62, 68, 75, 76, 80], and [82]; some robust (or hybrid of stochastic and robust) approaches that effective handle the seasonality of biomass are given by [39, 72], and [75].

The direct use of off-the-shelf solvers is the most common solution approach employed for solving proposed models for this problem that is generally of large-scale and is not easily solvable to optimality. For this reason, the problem is invariably recast by overly aggregating the input data, while sometimes customized exact or approximate algorithms are developed to solve these large-scale instances. For the sake of brevity, we do not present the details of these methods here, and instead, direct the reader to Sun et al. [79] for a thorough review of the decomposition-based solution methodologies. Benders [18] decomposition and partition approaches to solve large-scale mixed-integer programming formulations are presented in [19]. [64] uses a similar decomposition method to solve a stochastic optimization problem of

Table 1 Modeling approaches and key references from the literature

Modeling approaches	Key References
Linear Programming	Cundiff et. al. [27], Frombo et. al. [36], Flisberg et. al. [37], Gilani et. al. [39], Ren et. al. [69]
Nonlinear Programming	Bai et. al. [13], Bai et. al. [15], Bowling et. al. [20], Chen et. al. [24], Shabani et. al. [73]
Mixed-Integer Linear Programming	Aboytes-Ojeda et. al. [1], Aguayo et. al. [3], Aguayo et. al. [4], Akgul et. al. [5], Awudu et. al. [9], Bai et. al. [11], De Jong et. al. [29], De Mol et. al. [31], Dunnett et. al. [33], Dunnett et. al. [34], Gunnarsson et. al. [40], Judd et. al. [43], Kim et. al. [44], Lam et. al. [47], Laporte and Louveaux [48], Mapemba et. al. [54], Mapemba et. al. [55], Shastri et. al. [77], Sun et. al. [81], Üster et. al. [82], Zarei et. al. [88], Zhang et. al. [90], Zhang et. al. [91], Zhu et. al. [93], Zuo et. al. [94], This paper
Mathematical Programming under Uncertainty	Akhtari et. al. [6], Awudu et. al. [9], Azadeh et. al. [10], Babazadeh et. al. [11], Bairamzadeh et. al. [16], Balaman et. al. [17], Castillo-Villar et. al. [22], Chen et. al. [23], Cundiff et. al. [27], Dal -Mas et. al. [28], Gebreslassie et. al. [38], Huang et. al. [42], Kim et. al. [44], Marufuzzaman et. al. [56], Memişoğlu et. al. [58], Nur et. al. [62], Poudel et. al. [65], Poudel et. al. [66], Quddus et. al. [68], Ren et. al. [69], Savoji et. al. [72], Shabani et. al. [74], Shabani et. al. [75], Sharma et. al. [76], Sun et. al. [80], Zamar et. al. [86]
Multi-objective Mathematical Programming	Babazadeh et. al. [11], Bairamzadeh et. al. [16], Balaman et. al. [17], Cambero et. al. [21], Cucek et. al. [25], Gebreslassie et. al. [38], Liu et. al. [50], Malladi et. al. [53], Mavrotas et. al. [57], Miret et. al. [60], Shabani et. al. [74], You et. al. [84], Yue et. al. [85], Zamboni et. al. [87]

a multi-reservoir hydroelectric system. A two-stage stochastic programming model for the design and management of a biomass co-firing supply chain network under feedstock supply uncertainty is solved using a hybrid decomposition approach in [65]. The authors combined sample average approximation method with an enhanced progressive hedging algorithm to develop this hybrid approach. A biomass feedstock logistics problem with features similar to ours is solved using a typical two-stage Benders decomposition approach in [43]. In this regard, we develop a nested Benders decomposition strategy that disintegrates the problem on-hand into multiple well-known sub-problems like the Capacitated Vehicle Routing Problem (CVRP), and the Traveling Salesman Problem (TSP). Since the problem is so large, even these advanced methodologies struggle to provide optimal solutions. To somewhat counter this, a variety of cuts and bound improving techniques are used that can lead to faster convergence. [45] presents a set of improved bounds for a variant of multi-depot vehicle routing problem. We improved our solution methodology by proposing a multi-cut version of optimality cuts proposed by Laporte and Louveaux [48] in their integer L-shaped method for stochastic-integer programs. The L-shaped integer-method-based Benders optimality cuts are not new to the literature. The L-shaped method, originally proposed for two-stage stochastic linear programs, is a decomposition algorithm that exploits the block-angular structure of the

extensive form. It approximates the nonlinear expected recourse function using a piecewise linear outer approximation by iteratively adding optimality cuts. Laporte and Louveaux [48] extended the L-shaped method to stochastic programs with integer first-stage variables. Their key contribution was a new family of optimality cuts that provide a valid under-approximation of the expected recourse function when the first-stage variables are binary. This family of optimality cuts involves standard integer optimality cuts and subgradient-based cuts [8]. also proposed an improvement to the integer L-shaped method by introducing an alternating cut strategy that avoids expensive evaluations of the recourse function, as well as a new family of cuts derived from a Lagrangian relaxation. They used this family of L-shaped cuts and presented a new alternating-cut strategy that reduces the overall computation effort of the stochastic program that they consider. While their focus was primarily on avoiding expensive recourse function evaluations and improving the convergence of multi-stage stochastic linear programs with recourse, our focus is to apply the proposed optimality cuts to a large-scale deterministic problem and improve convergence of our solution methodology (Nested Benders Decomposition strategy). The novelty in our approach is in directly handling the integrality in generating these integer optimality cuts, which resulted in faster convergence for our large-scale deterministic problem. The faster convergence is attributed to our proposed optimality cuts that can capture solution value at an integer solution for the sub-problem(s). This computational advantage is evident from the results of our detailed investigation discussed in Section-5.2. In addition, we demonstrate that our proposed optimality cuts are valid, feasible, and tighter than those proposed by Laporte and Louveaux [48]. The finer details related to the construction of such optimality cuts and the relevant literature regarding our solution methodology, along with our proposed optimality cuts, are extensively explored in Sect. 4, titled 'Solution Methodology—Nested Benders Decomposition', and its Sub-Sect. 4.1, titled 'Optimality Cuts'.

As alluded to earlier as well, to the best of our knowledge, the problem considered in this paper hasn't been studied with the feature of routing of load-out equipment among the SSLs. This feature adds to the complexity of the problem. Our research addresses this gap by proposing a mixed-integer programming formulation that effectively accommodates this feature and an exact solution methodology that provides optimal solutions to the real-life size problem instances. The proposed Nested Benders decomposition algorithm is applied to decompose the large-scale problem on hand to effectively handle the decision making in multiple stages (sub problems and sub-subproblems). We acknowledge that there are several approximation approaches (for example see [70]) like meta-heuristics, search-based algorithms, etc., developed in the literature that has been applied to similar biomass supply chain problems. But it is a different solution approach. Moreover, it is not possible to prove performance guarantee for such a method even though it may, in some cases, give decent acceptable solutions. For this reason, we compare our algorithm with the state-of-the-art MIP solver CPLEX®'s Branch-and-Bound and Benders Strategy algorithms. We show that our proposed algorithm converges significantly faster than the CPLEX® algorithms. In addition, it guarantees optimal solutions for all considered problem instances in a very reasonable amount of time.

The remainder of this paper is organized as follows. In Sect. 2.1, we highlight our contributions to the relevant literature. In Sect. 3, we present the model formulation for the biomass feedstock logistics problem. Section 4 presents our exact solution methodology i.e., Nested Benders decomposition algorithm and a novel set of optimality cuts (Sect. 4.1) that aid in convergence and provide optimal solutions to the real-life size problem instances. Section 5 consists of the results and analysis of a thorough computational investigation. Based on the analysis, the efficacy and superiority of our solution methodology is demonstrated over the

state-of-the-art CPLEX® Solver algorithms. Lastly, in Sect. 6, we conclude and share a few possible future extensions of the presented work.

2.1 Contributions

There are the following contributions of our work:

(i) As alluded to above, we consider the routing of load-out equipment among the SSLs. This feature has not been explicitly considered in the work presented in the literature. Thus, it adds a feature that is important for reducing biomass feedstock logistics cost.
(ii) Our problem involves three echelons of logistics, namely, from production fields to SSLs, from SSLs to biocrude plants, and from biocrude plants to the refinery. We adopted a nested Benders decomposition algorithm, which is typically used to handle stochastic problems, for the solution of the underlying deterministic logistics problem.
(iii) The implementation of our proposed nested Benders decomposition algorithm for the deterministic case involves binary variables in the subproblems. Therefore, a novelty of our approach is in directly handling the integrality in generating integer optimality cuts that are tighter than those presented in the literature.
(iv) We have demonstrated the efficacy of the proposed nested Benders decomposition algorithm by applying it to large real-life size problem instances. We also show that the proposed Benders decomposition algorithm outperforms the state-of-the-art CPLEX® Branch-and-Bound and CPLEX® Benders Strategy algorithms.

3 Model formulation

In this section, we first present the notations and some important assumptions. We then present the formulation of the Biomass Logistics Problem as Model BLP. Below are some notations to state the assumptions (Table 2).

The assumptions are as follows: (1) Each potential BeP location, $l \in L$, operates with its own mutually exclusive set of fields (I_l), SSLs (J_l), and equipment systems/tours (T_l). (2) An SSL, $j \in J$, is only permitted to procure biomass from the fields that lie within a prespecified radius around it. This set of fields is denoted by NI_j. Similarly, NJ_i represents the set of all the SSLs that can be accessed by field $i \in I$.

Some more notations including the parameters and decision variables are given in Table 3.

We denote the objective function value of a model formulation, m, by $g(m)$. Also, a model and its corresponding decision variables are notated by a superscript '', whenever the

Table 2 Notations-sets

L	Set of potential BePs
I	Set of potential fields
J	Set of potential SSLs
T	Set of tours (a single route over the SSLs assigned to an equipment system is referred to as a tour, and is denoted by t)
NI_j	Set of all the fields that lie within a specified radius of SSL $j \in J$
NJ_i	Set of all the SSLs that can be accessed by field $i \in I$

Table 3 Notations-parameters and decision variables

Parameters:	
f_{ijl}	Cost for transporting all of biomass from field i to BeP l through SSL j
d_l	Per unit cost for transporting biomass from BeP l to the refinery
c_{jk}	Total cost for moving an equipment system from SSL j to SSL k
e_0	Annual cost of an equipment system
sc	Fixed setup/take-down cost of an equipment system
rc	Annual land rental fee (per Mg of biomass stored on it) for the SSLs
ha_i	Size of production field i (in hectares)
$s_{[\min]}$	Minimum size of an SSL (e.g., 3 days' worth of unloading in hectares)
$s_{[\max]}$	Maximum size of an SSL (e.g., 30 days' worth of unloading in hectares)
$E_{[\max]}$	Maximum processing capacity of each equipment system/tour (in hectares)
$BeP_{[\min]}$	Minimum amount of biomass (in hectares) to be processed at each BeP
bep_l	Annual amount of biomass (in hectares) processed at BeP l
R	Annual biomass requirement at the refinery (in hectares). (Note: For the sake of convenience, the requirement at the refinery is also expressed in hectares)
Decision variables:	
y_{ij}	$= 1$, if field i transports biomass to SSL j; 0, otherwise
y_{ijt}	$= 1$, if field i transports biomass to SSL j which is allocated to tour t; 0, otherwise
q_l	$= 1$, if BeP l is utilized; 0, otherwise
z_j	$= 1$, if SSL j is utilized; 0, otherwise
z_{jt}	$= 1$, if SSL j is utilized and is allocated to tour t; 0, otherwise. Note that, z_{0t} is used to indicate if tour t is utilized or not
aux_l	auxiliary variables in the nested-Benders-decomposition-based model
x_{jkt}	$= 1$, if SSL k is preceded by SSL j on tour t associated with an equipment system; 0, otherwise
u_{jt}	Order/ranking variable for SSL j on tour t
w_{jt}	auxiliary variables used to eliminate subtours (under the assumption that there is no fixed depot while routing equipment systems)

model is solved by relaxing the integrality constraints. For example, $g(\text{BLP-SSP}'_l)$ denotes the objective function value of the relaxed Model BLP-SSP$_l$.

Next, we present Model BLP for the Biomass Logistics Problem.

Model BLP:

Minimize:

$$2sc\sum_{l\in L}\sum_{j\in J_l} z_j + \sum_{l\in L}\sum_{j\in J_l}\sum_{i\in NI_j} f_{ijl}y_{ij} + rc\sum_{l\in L}\sum_{j\in J_l}\sum_{i\in NI_j} ha_i y_{ij}$$
$$+\sum_{l\in L} d_l bep_l + e_0\sum_{l\in L}\sum_{t\in T_l} z_{0t} + 2\sum_{l\in L}\sum_{j\in J_l}\sum_{k\in J_l, k\neq j}\sum_{t\in T_l} c_{jk}x_{jkt} \quad (1.1)$$

Subject to:

$$z_j \le q_l,\ \forall j \in j_l,\ l \in L \tag{1.2}$$

$$y_{ij} \le z_j,\ \forall i \in NI_j,\ j \in J \tag{1.3}$$

$$\sum_{j \in NJ_i} y_{ij} \le 1,\ \forall i \in I \tag{1.4}$$

$$\sum_{i \in NI_j} ha_i y_{ij} \ge s_{[\min]} z_j,\ \forall j \in J \tag{1.5}$$

$$\sum_{i \in NI_j} ha_i y_{ij} \le s_{[\max]} z_j,\ \forall j \in J \tag{1.6}$$

$$bep_l = \sum_{j \in J_l} \sum_{i \in NI_j} ha_i y_{ij} \ge BeP_{[\min]} q_l,\ l \in L \tag{1.7}$$

$$\sum_{l \in L} bep_l \ge R \tag{1.8}$$

$$bep_l \le |T_l| E_{[\max]},\ \forall l \in L \tag{1.9}$$

$$y_{jj} = z_j,\ \forall j \in J \tag{1.10}$$

$$\sum_{t \in T_l} z_{jt} = z_j, \quad \forall j \in J_l,\ l \in L \tag{1.11}$$

$$z_{jt} \le z_{0t},\ \forall j \in J_l,\ t \in T_l, \quad l \in L \tag{1.12}$$

$$\sum_{t \in T_l} y_{ijt} = y_{ij}, \quad \forall j \in J_l,\ i \in NI_j,\ l \in L \tag{1.13}$$

$$y_{ijt} \le z_{jt},\ \forall j \in J_l,\ i \in NI_j, \quad t \in T_l, \quad l \in L \tag{1.14}$$

$$\sum_{j \in J_l} \sum_{i \in NI_j} ha_i y_{ijt} \le E_{[\max]}, \quad \forall t \in T_l,\ l \in L \tag{1.15}$$

$$\sum_{j \in J_l,\ j \ne k} x_{jkt} = z_{kt}, \quad \forall k \in J_l,\ t \in T_l,\ l \in L \tag{1.16}$$

$$\sum_{j \in J_l,\ j \ne k} x_{kjt} = z_{kt}, \quad \forall k \in J_l,\ t \in T_l,\ l \in L \tag{1.17}$$

$$\sum_{j \in J_l} w_{jt} = z_{0t}, \quad \forall t \in T_l,\ l \in L \tag{1.18}$$

$$w_{jt} \le z_{jt},\ \forall j \in J_l,\ t \in T_l, \quad l \in L \tag{1.19}$$

$$j^- w_{j^-,t} \ge j w_{jt},\ \forall j \in J_l \backslash J_l^1, \quad t \in T_l,\ l \in L \tag{1.20}$$

$$\begin{aligned} &u_{jt} - u_{kt} - |J_l| \left(w_{jt} + w_{kt}\right) + |J_l| x_{jkt} + (|J_l| - 2) x_{kjt} \\ &\le |J_l| - 1,\ \forall j \in J_l,\ k \in J_l,\ k \ne j,\ t \in T_l,\ l \in L \end{aligned} \tag{1.21}$$

$$u_{jt} \ge z_{jt} - w_{jt}, \quad \forall j \in J_l,\ t \in T_l,\ l \in L \tag{1.22}$$

$$u_{jt} \le \sum_{k \in J_l} z_{kt} - z_{0t}, \quad \forall j \in J_l,\ t \in T_l,\ l \in L \tag{1.23}$$

$$q_l \in \{0, 1\}, \quad bep_l \geq 0, \forall l \in L \tag{1.24}$$

$$z_j \in \{0, 1\} \quad \forall j \in J \tag{1.25}$$

$$y_{ij} \in \{0, 1\} \forall j \in J, \quad i \in NI_j \tag{1.26}$$

$$z_{jt} \in \{0, 1\} \forall j \in J_l \cup \{0\}, \quad t \in T_l, l \in L \tag{1.27}$$

$$y_{ijt} \in \{0, 1\} \forall j \in J_l, i \in NI_j, \quad t \in T_l l \in L \tag{1.28}$$

$$x_{jkt} \in \{0, 1\} \forall j \in J_l, k \in J_l, \quad k \neq j, \quad t \in T_l l \in L \tag{1.29}$$

$$u_{jt} \geq 0 \forall j \in J_l, \quad t \in T_l l \in L \tag{1.30}$$

$$w_{jt} \in \{0, 1\} \forall j \in J_l, \quad t \in T_l l \in L \tag{1.31}$$

The objective function in (1.1) consists of equipment systems' setup cost, biomass transportation cost from fields to BePs (for in-field hauling from each field to an SSL and for hauling by trailer/trucks from each SSL to a BeP subsequently), SSLs' rental cost, biomass transportation cost from BePs to the refinery, equipment ownership cost, and travel cost for routing equipment systems among SSLs, respectively. A factor of 2 is used in the first and the last terms because of the assumption of two setups and two sets of routings in a tour resulting from two harvesting seasons in a year. Constraints (1.2) assert a BeP to be utilized only if it is used. Similarly, Constraints (1.3) assert a field to be allocated to an SSL only if it is utilized. Constraints (1.4) capture the fact that every production field is allocated to at most one SSL. Constraints (1.5) and (1.6) provide a lower and an upper bound, respectively, on the size of each SSL. Constraints (1.7) capture the amount of biomass processed at each BeP and the fact that it must satisfy a lower bound on this amount. Constraints (1.8) ensure that enough biomass is collected through all the BePs to fulfil a fixed annual requirement at the refinery. Constraints (1.9) provide an upper bound on the amount of biomass processed at each BeP, based on the total capacity of all the equipment systems combined. Constraint (1.10) ensures that the biomass from a field that is used for the development of an SSL is allocated to that SSL itself if used. Constraints (1.11) allow at most one tour to be allocated to an SSL if used. Constraints (1.12)—(1.14) assert a tour/equipment system to be utilized only if it is used for loading biomass at least one of the SSLs. Constraints (1.15) ensure tour balancing by restricting the maximum amount of biomass that a single equipment system can process. Constraints (1.16) and (1.17) are degree constraints for the underlying TSP for each tour. Constraints (1.18) and (1.19) ensure that exactly one SSL is considered to act as a makeshift depot for a given tour so that the other SSLs that belong to the same tour do not form a subtour. This is ensured by Subtour Elimination Constraints (1.21) that were first proposed by Miller et al. [59] (and they are popularly known as MTZ SECs), and subsequently tightened by Desrochers and Laporte [32]. We modify the MTZ SECs to incorporate the requirement that there is no fixed depot in any tour. Constraints (1.20) are symmetry-breaking constraints, where j^- is the predecessor of j and J_l^1 is the first element of J_l (see [45]). Constraints (1.22) and (1.23) not only provide lower and upper bounds on the ranking variables, respectively but also tighten the LP convex hull of the formulation. Constraints (1.24)—(1.31) impose logical restrictions on the decision variables.

4 Solution methodology-nested benders decomposition

In this section, present the decomposition methodology used to solve this problem. Since the model is relatively large, an efficient way in general is to somehow decompose it. Although there are several established solution techniques available in the literature like Column Generation, Dantzig-Wolfe Reformulation, etc. among others, we apply Benders Decomposition to take the advantage of nesting (multiple stage decomposition -decomposing subproblems further into sub-subproblems; discussed in detail ahead). For faster convergence, we then develop some optimality cuts for our formulation. These proposed optimality cuts are a new multi-cut version of Laporte and Louveaux's [48] family of optimality cuts. We show that the proposed cuts are stronger than those proposed by Laporte and Louveaux [48] by proving its validity, feasibility, and tightness. Lastly, we present a 'Nested Benders Decomposition' algorithm and a flowchart illustrating the steps involved in the decomposition scheme for ease of interpretation.

In a conventional application of the Benders decomposition technique [18], a series of master and sub-problems are solved iteratively. The master problem is a relaxation of the original formulation obtained by removing some constraints and is solved to obtain an initial solution. A sub-problem that typically represents the dual, or pricing, of the relaxed constraints is solved to generate a (Benders) cut if either the whole problem has not converged to within a desired MIP optimality gap value or the current master problem solution is violated. This constraint is added to the master problem, which is then re-solved. This process is continued until the master problem and the sub-problem converge to an optimal solution or are within a desired MIP optimality gap value. Since the constraints are relaxed and are iteratively added to the master problem, Benders decomposition technique is also known as a relaxation strategy.

We extend the Benders decomposition method (that involves two stages) to a scheme that has three stages, and hence, call it a Nested Benders decomposition (NBD) method. Louveaux [51] first performed an outer linearization built on the two-stage L-shaped method or the Benders decomposition method for multistage quadratic problems. Birge [19] extended the two-stage method to the linear case. This approach also appears in Pereira and Pinto [64]. Almost the entire literature on the NBD method is devoted to multistage stochastic problems. However, we apply this approach to a deterministic problem, specifically, to enable Model BLP to solve real-life-sized problem instances. As also noted earlier, the novelty of our work is in dealing with a MIP program in the sub-problem. In our proposed decomposition scheme, the sub-problems are solved as integer programs rather than as their LP relaxations. We also employ a new multi-cut version of the Benders optimality cuts proposed by Laporte and Louveaux [48]. Our proposed optimality cuts can capture solution value at an integer solution for the sub-problem(s). This variation is described later in Sub-Sect. 4.1 titled 'Optimality Cuts'.

Next, we describe the nested Benders decomposition method to solve Model BLP. The first stage of this method, called the master problem, is referred to as Model BLP-MP. It concerns the selection of BePs, SSLs and fields, and the assignment of chosen fields to SSLs. The decision variables involved in Model BLP-MP are y_{ij}, $\text{au}x_l$, z_j, bep_l, and q_l. For a given solution to Model BLP-MP, the remaining problem is separable over individual BePs, and essentially becomes a *Capacitated Vehicle Routing Problem (CVRP)*. We chose to solve it by further decomposing it into two stages. Thus, for a given solution to Model BLP-MP, and l^{th} BeP, the second stage is referred to as Model BLP-SP$_l$. It concerns the assignment of SSLs to tours (Note: A tour belongs to a single set of equipment systems that is routed over

the SSLs pre-assigned to it). The decision variables involved in Model BLP- SP$_l$ are y_{ijt}, and z_{jt}. Given a solution to Model BLP-SP$_l$, the third stage, referred to as Model BLP-SSP$_l$, is essentially a collection of multiple yet separable Traveling Salesman Problems (TSPs), each of which determines a sequence in which an equipment system is routed over a set of SSLs predesignated to it to form a tour, but with a variant that no tour has a fixed depot. Each tour is repeated twice since each SSL is visited twice by the same equipment system due to a bi-annual harvesting season. The decision variables involved in Model BLP-SSP$_l$ are x_{jkt}, u_{jt}, and w_{jt} or b_{jt} as described below. Next, we present Model BLP-MP.

Model BLP-MP:

$$MPC: Minimize 2sc \sum_{l\in L}\sum_{j\in J_l} z_j + \sum_{l\in L}\sum_{j\in J_l}\sum_{i\in NI_j} f_{ijl}y_{ij} + rc\sum_{l\in L}\sum_{j\in J_l}\sum_{i\in NI_j} ha_i y_{ij} + \sum_{l\in L} d_l bep_l + \sum_{l\in L} SPC_l \tag{2.1}$$

Subject to:

$$\{\text{Constraints}(1.2) - (1.10),\ (1.24) - (1.26)\} \tag{2.2}$$

$$aux_l\left(E_{[\max]}\right) \geq bep_l,\ \forall l \in L \tag{2.3}$$

$$\text{au}x_l \in \mathbb{Z}^+,\ \forall l \in L \tag{2.4}$$

SPC_l captures the cost of Model BLP-SP$_l$ in Model BLP-MP. The costs relevant for Model BLP-MP consist of the sum total of SSLs' equipment setup cost, biomass transportation cost from fields to BeP l (in-field hauling from fields to SSLs and by trailer/truck from SSLs to the BeP l subsequently), SSLs' usage/development cost, and the biomass transportation cost from BeP l to the refinery. In lieu of Constraints (1.9), since the tours are determined in the subproblem BLP-SP$_l$, we use a variable aux_l to serve as a proxy for $|T_l|$ and the Constraints (1.3). Model BLP-SP$_l$ is as follows:

Model BLP-SP$_l$ ($q_l = 1$):

$$SPC_l: Minimize\ e_0 \sum_{t\in T_l} z_{0t} + SSPC_l \tag{2.5}$$

Subject to:

$$\sum_{t\in T_l} z_{jt} = z_j,\ \forall j \in J_l \qquad \leftarrow \alpha_j \tag{2.6}$$

$$\sum_{t\in T_l} z_{0t} \geq aux_l \qquad \leftarrow \beta_l \tag{2.7}$$

$$z_{jt} \leq z_{0t} \forall j \in J_l \qquad t \in T_l \tag{2.8}$$

$$\sum_{t\in T_l} y_{ijt} = y_{ij}, \qquad \forall i \in NI_j, j \in J_l \qquad \leftarrow \gamma_{ij} \tag{2.9}$$

$$y_{ijt} \leq z_{jt},\ \forall i \in NI_j,\ t \in T_l, \qquad j \in J_l \tag{2.10}$$

$$\sum_{j\in J_l}\sum_{i\in NI_j} ha_i y_{ijt} \leq E_{[\max]},\ \forall t \in T_l \qquad \leftarrow \delta_t \tag{2.11}$$

$$z_{0t} \geq 0 \forall t \in T_l \tag{2.12}$$

$$z_{jt} \geq 0 \forall j \in J_l, \qquad \in T_l \tag{2.13}$$

$$y_{ij} \geq 0 \forall i \in NI_j, \qquad j \in J_l \tag{2.14}$$

$$z_{0t} \in \{0, 1\} \qquad \forall t \in T_l \tag{2.15}$$

$$z_{jt} \in \{0, 1\} \quad \forall j \in J_l, t \in T_l \tag{2.16}$$

$$y_{ijt} \in \{0, 1\} \quad \forall i \in NI_j, t \in T_l, j \in J_l \tag{2.17}$$

The cost term '$SSPC_l$' in (2.5) captures the cost of Model BLP-SSP$_l$ in Model BLP-SP$_l$. Constraints (2.3), (2.4), and (2.7) together enforce $\sum_{t \in T_l} z_{0t} \geq \frac{bep_l}{E_{[\max]}}$, $\forall l \in L$. For practical purposes, the size of Constraints (2.10) presents a heavy computational burden. Thereby, although it is well-known that the disaggregated version (2.10) provides a stronger bound, we drop (2.10) in favor of their aggregated version as given in Constraints (2.18).

$$\sum_{i \in NI_j} y_{ijt} \leq \left|NI_j\right| z_{jt}, \forall j \in J_l, t \in T_l \tag{2.18}$$

We add symmetry-breaking constraints to Model BLP-SP$_l$ in the form of (2.19)—(2.25), which enforce that the maximum index among all SSLs assigned to a tour follows an increasing order with tour indices. This results in faster convergence between the SP and SSP stages.

$$b_{jt} \leq 1, \forall j \in J_l, t \in T_l \qquad \leftarrow \epsilon_{jt} \tag{2.19}$$

$$v_t \geq j z_{jt}, \forall j \in J_l, \qquad t \in T_l \tag{2.20}$$

$$v_{t^-} \leq v_t, \qquad \forall t \in T_l \backslash T_l^1 \tag{2.21}$$

$$v_t \leq j z_{jt} + \left(\max_{j \in J_l}\{j\}\right)\left(1 - b_{jt}\right), \qquad \forall j \in J_l, t \in T_l \qquad \leftarrow \zeta_{jt} \tag{2.22}$$

$$\sum_{j \in J_l} b_{jt} \geq 1, \qquad \forall t \in T_l \qquad \leftarrow \eta_t \tag{2.23}$$

$$b_{jt} \geq 0, \forall j \in J_l, t \in T_l \tag{2.24}$$

$$b_{jt} \in \{01\}, \forall j \in J_l, \qquad t \in T_l \tag{2.25}$$

Note that Constraints (2.19) bound the variables, b_{jt}, from above, and hold meaning only when Model BLP-SP$_l$ is solved as relaxed and the dual values are non-zero.

In view of symmetry breaking constraints 2.19–2.25 used in Model BLP-SP$_l$,b_{jt} can be used in place of w_{jt} in deciding makeshift depot for a tour. Note that, this will also eliminate the use of symmetry-breaking Constraints (1.20) for w_{jt}, since the choice ofb_{jt} being unity is already implied uniquely by Constraints 2.19–2.25 for each tour.

We now present Model BLP-SSP$_l$, wherein Constraints 1.18–1.23 and (1.31) are replaced by Constraints 2.29–2.31.

Model BLP-SSP$_l$ ($q_l = 1$):

$$SSPC_l : Minimize \qquad 2 \sum_{j \in J_l} \sum_{k \in J_l, k \neq j} \sum_{t \in T_l} c_{jk} x_{jkt} \tag{2.26}$$

Subject to:

$$\sum_{j\in J_l,\, j\neq k} x_{jkt} = z_{kt},\ \forall k \in J_l,\ t \in T_l \qquad \leftarrow \theta_{kt} \tag{2.27}$$

$$\sum_{j\in J_l,\, j\neq k} x_{kjt} = z_{kt},\ \forall k \in J_l,\ t \in T_l \qquad \leftarrow \iota_{kt} \tag{2.28}$$

$$\begin{aligned} &u_{jt} - u_{kt} + |J_l| x_{jkt} + (|J_l| - 2) x_{kjt} \\ &\leq |J_l| - 1 + |J_l| \left(b_{jt} + b_{kt}\right),\ \forall j \in J_l,\ k \in J_l,\ k \neq j,\ t \in T_l \qquad \leftarrow \kappa_{jkt} \end{aligned} \tag{2.29}$$

$$u_{jt} \geq z_{jt} - \left(b_{jt} + z_{0t} - 1\right),\ \forall j \in J_l,\ t \in T_l \qquad \leftarrow \lambda_{jt} \tag{2.30}$$

$$u_{jt} \leq \sum_{k\in J_l} z_{kt} - z_{0t},\ \forall j \in J_l,\ t \in T_l \qquad \leftarrow \mu_{jt} \tag{2.31}$$

$$x_{jkt} \geq 0,\ \forall j \in J_l,\ k \in J_l,\ k \neq j,\ t \in T_l \tag{2.32}$$

$$x_{jkt} \in \{0, 1\},\ \forall j \in J_l,\ k \in J_l,\ k \neq j,\ t \in T_l \tag{2.33}$$

$$u_{jt} \geq 0,\ \forall j \in J_l,\ t \in T_l \tag{2.34}$$

The proposed nested Benders decomposition algorithm is given in Algorithm 1. For convenience we have presented its flowchart in Fig. 1. It works as follows:

The overall procedure comprises inner and outer loops as outlined by two boxes in Fig. 1. First, the first-stage problem (BLP-MP), referred to as the Master Problem, is solved to obtain a feasible solution (say, s_1) that constitutes a lower bound LB. Using the feasible solution (s_1, LB), we solve the sub-problems BLP-SP$_l$, and BLP-SSP$_l$ for each BeP $l \in L$. More specifically, the second stage involves solving the sub-problem BLP-SP$_l$ to get a second-stage feasible solution (say, s_2) and a lower bound LB^{SP_l}. Using the second-stage feasible

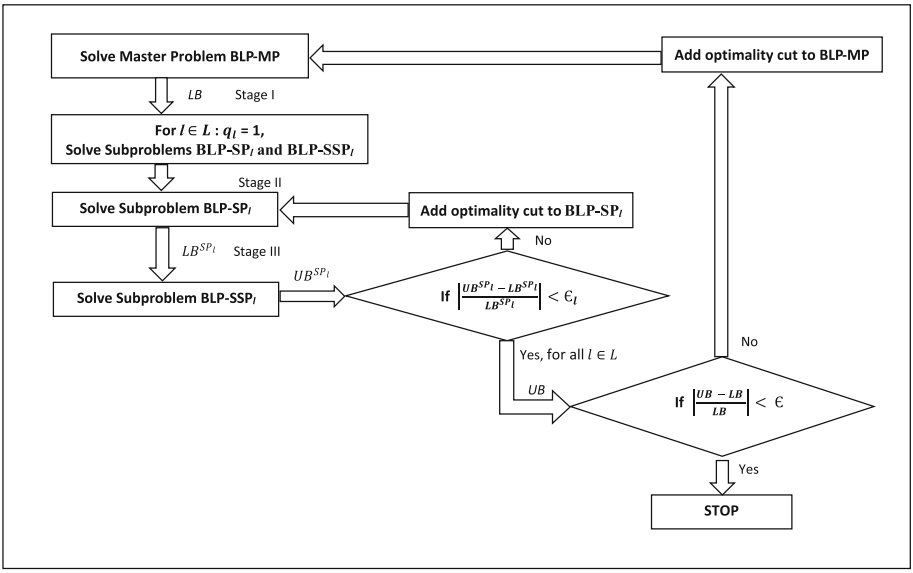

Fig. 1 Nested Benders Decomposition methodology flowchart

solution $\left(s_2,\ LB^{SP_l}\right)$, we solve the third-stage sub-problem BLP-SSP$_l$ to get an upper bound UB^{SP_l}. This step is repeated until the desired optimality gap $\left|\frac{UB^{SP_l}-LB^{SP_l}}{LB^{SP_l}}\right|$ is achieved for all $l \in L$. An optimality cut is added to Model BLP-SP$_l$ whenever the optimality gap value doesn't meet the desired tolerance value. (Note that the optimality cuts mentioned in Fig. 1 and Algorithm 1 below are discussed in detail in the next Sect. 4.1). The procedure then moves to the outer loop. A similar iterative process of adding cuts is followed for the first-stage Master Problem BLP-MP until the MP-SP optimality gap is within the set optimality tolerance value.

1: Initialize: $LB, UB, LB^{SP_l}, UB^{SP_l}$
2: **while** $\left|\frac{UB\ -LB}{LB}\right| > \epsilon$ (i.e., MP optimality gap is not satisfied) **do**
3: add optimality cut to BLP-MP
4: /* LB **lower bound update** */
5: $LB \leftarrow$ solve BLP-MP
6: **for** $l \in L:\ q_l = 1$
7: **while** $\left|\frac{UB^{SP_l}-LB^{SP_l}}{LB^{SP_l}}\right| > \epsilon_l$ (i.e., SP$_l$ optimality gap is not satisfied) **do**
8: add optimality cut to BLP-SP$_l$
9: /* SP_l **lower bound update** */
10: $LB^{SP_l} \leftarrow$ solve BLP-SP$_l$
11: solve BLP-SSP$_l$ using LB^{SP_l}
12: /* SP_l **upper bound update** */
13: $UB^{SP_l} \leftarrow$ BLP-SSP$_l$ solution
14: **end while**
15: **end for**
16: /* UB **upper bound update** */
17: $UB \leftarrow UB^{SP_l}$
18: **end while**

Algorithm 1: Nested Benders Decomposition

4.1 Optimality cuts

As also noted earlier, Laporte and Louveaux [48] derived optimality cuts for problems wherein the second-stage variables are integer/binary, with the first stage containing binary decision variables only, a setting that is similar to that in our case (where the input solutions to the second-stage and the third-stage integer sub-problems are a set of binary decision variables of the first-stage and second-stage problems, respectively). Our optimality cuts are multi-cut strengthening of the integer optimality cuts proposed by Laporte and Louveaux [48]. We show this in Proposition 1 below. The key difference lies in considering an expanded neighborhood of the current solution in determining a lower bound.

Towards this end, we first introduce the relevant notation and equations necessary to represent the optimality cut (referred to as "Improved optimality cut") given in Proposition

6 of Laporte and Louveaux [48], which we reproduce as follows:

$$\theta \geq a\left(\sum_{i\in S_r} \boldsymbol{x}_i - \sum_{i\in \overline{S}_r} \boldsymbol{x}_i\right) + \theta_r - a|S_r| \tag{2.35}$$

where, $\boldsymbol{x}$ denotes a general solution to the Stage 1 master problem, which serves as input to the second stage sub-problem. Please note that $\boldsymbol{x}$ in (2.35) is different from $\boldsymbol{x}$ defined in the BLP formulation (Sect. 3). S_r and $\overline{S}_r$ are the sets of variable indices for which $x_i = 1$ and $x_i = 0$, respectively, in the current solution, $\boldsymbol{x}^r$, at the r^{th} iteration. Here θ, in general, is an approximation to $Q(\boldsymbol{x})$ (i.e., the expected value of the objective function over the second-stage sub-problems with integer/binary variables) for a given $\boldsymbol{x}$, whereas θ_r denotes the true value of the second stage, $Q(\boldsymbol{x}^r)$, at the current solution. Further, let $N_r\ (s)$ define the set of solutions that constitute 's-neighbors' (s varies from 1 to $|S_r| + \left|\overline{S}_r\right|$), such that $\sum_{i\in S_r} \boldsymbol{x}_i - \sum_{i\in \overline{S}_r} \boldsymbol{x}_i = |S_r| - s$. Note that, Laporte and Louveaux [48] consider $\boldsymbol{x}$ to be a multi-dimensional binary variable; as such, $s = 0 \Leftrightarrow \boldsymbol{x} = \boldsymbol{x}^r$. Let, $\lambda_r(s)$ denote a lower bound on $\min_{\boldsymbol{x}\in N_r(s)}\{Q(\boldsymbol{x})\}$ and L denote an overall lower bound on $Q(\boldsymbol{x})$. The value of a is given by, $a = \max\{\theta_r - \lambda_r(1),\ (\theta_r - L)/2\}$.

Note that, by the definitions of $\lambda_r(s)$ and L, their selection is arbitrary and is usually problem dependent. Understandably, the authors have not prescribed any rigorous methodology for computing them uniquely. However, they do prescribe certain steps that could be used to compute these lower-bound estimates in a general case. Before we describe how to compute these lower bound estimates, we must point out that Laporte and Louveaux [48] considered a stochastic integer program with complete recourse, whereas, we deal with a deterministic case in our work. For a fair comparison, therefore, we fix the variable representing the probability distribution to be uni-variate, thereby, considering only a single sub-problem at Stage 2 for every master problem solution in their work. We reproduce a lower bound on $Q(\boldsymbol{x})$ under such an assumption (following Eq. (17) in their work) as follows:

$$L = \underset{\boldsymbol{x},\lambda}{min}\{\lambda|\boldsymbol{x} \in \boldsymbol{X} \text{ and } (\lambda, \boldsymbol{x}) \text{ follows Equation(2.37) for } k = 1, \ldots, s\}\,, \tag{2.36}$$

for any finite value $s \geq 1$. Here, $\boldsymbol{X}$ is the domain of all binary first-stage vectors of decision variables, i.e., $\boldsymbol{X} = \left\{\boldsymbol{x}\middle|A\boldsymbol{x} = b,\ \boldsymbol{x} = \{0,\ 1\}^{n1}\right\}$.

$$\lambda \geq R(\boldsymbol{x}) = R\left(\boldsymbol{x}^k\right) + \partial R\left(\boldsymbol{x}^k\right)\left(\boldsymbol{x} - \boldsymbol{x}^k\right) \tag{2.37}$$

where, $R(\boldsymbol{x}) = \min\{qy|Wy = h - T\boldsymbol{x},\ 0 \leq y \leq 1\}$, represents the continuous relaxation of $Q(\boldsymbol{x})$, and $\partial R\left(\boldsymbol{x}^k\right)$ is a sub-gradient of R at $\boldsymbol{x}^k$. Note that, the computation of L in Eq. (2.36) can either be performed in advance (whenever we can represent $Q(\boldsymbol{x})$ or $R(\boldsymbol{x})$ analytically as a function of $\boldsymbol{x}$, for all $\boldsymbol{x} \in \boldsymbol{X}$, which is only possible in problems with a special structure at second stage; however, such an analytic representation of second stage is not possible in our case), or by using the information available up until the r^{th} iteration in the scheme of Benders decomposition. Therefore, for a general case, we obtain L as follows:

$$L = \underset{\boldsymbol{x}\in\boldsymbol{X}}{min}\left\{\lambda\middle|\lambda \geq R\left(\boldsymbol{x}^k\right) + \partial R\left(\boldsymbol{x}^k\right)\left(\boldsymbol{x} - \boldsymbol{x}^k\right),\ \forall k = 1, \ldots, r\right\}. \tag{2.38}$$

Similarly, we compute $\lambda_r(s)$ as follows:

$$\lambda_r(s) = \underset{\boldsymbol{x}\in N_r(s)\subset\boldsymbol{X}}{min}\left\{\lambda\middle|\lambda \geq R\left(\boldsymbol{x}^k\right) + \partial R\left(\boldsymbol{x}^k\right)\left(\boldsymbol{x} - \boldsymbol{x}^k\right),\ \forall k = 1, \ldots, r\right\}. \tag{2.39}$$

Clearly, we have,$\lambda_r(s) \geq L$, $\forall s = 0, 1, \ldots, |S_r| + \left|\overline{S}_r\right|$. Even though we have described a general procedure to obtain $\lambda_r(s)$ for all s values, it is to be noted that the optimality cut proposed by Laporte and Louveaux [48] at the r^{th} iteration (as given by Eq. (2.35)) uses only $\lambda_r(1)$. Next, we decompose this cut into different cases depending upon the value of $\boldsymbol{x}$ as follows:

$$\theta \geq \begin{cases} \theta_r & \text{at } \boldsymbol{x} = \boldsymbol{x}^r \\ \theta_r - a = \lambda_r(1)^{\downarrow} & \forall \boldsymbol{x} \in N_r(1) \subset \boldsymbol{X} \\ \theta_r - 2a = L^{\downarrow} & \forall \boldsymbol{x} \in N_r(2) \subset \boldsymbol{X} \\ \theta_r - s \cdot a = L' < L & \forall \boldsymbol{x} \in N_r(3) \subset \boldsymbol{X} s \geq 3. \end{cases} \tag{2.40}$$

The symbol$\downarrow$ as an exponent denotes that the actual value is less than or equal to the base value (nonetheless, the cut remains valid). In the upcoming sections, we first describe our proposed *Optimality cuts* in detail and then discuss their validity, tightness, and feasibility.

Optimality cut from BLP-SSP$_l$to BLP-SP$_l$: For a given solution to Models BLP-SP$_l$ and BLP-SSP$_l$, if the SP-SSP optimality gap is not within the set optimality tolerance, τ^{sp}, i.e., $\left|\frac{g(BLPSSP_l)-SSPC_l}{SSPC_l}\right| > \tau^{sp}$, we add the following optimality cuts (at iteration ϕ) to Model BLP-SP$_l$. Note that the dual solution is obtained by solving Model BLP - SSP$'_l$.

$$\begin{aligned}
&SSPC_l \geq \mathrm{LB}_\phi \\
&= F\left(\boldsymbol{z}, \boldsymbol{b} \middle| \boldsymbol{z}^\phi, \boldsymbol{b}^\phi\right) + \left(g(\text{BLP - SSP}_l) - g\left(\text{BLP - SSP}'_l\right)\right) r^{sp}_{l\phi} \\
&\left(\begin{array}{l} \textit{where } F\left(\boldsymbol{z}, \boldsymbol{b} \middle| \boldsymbol{z}^\phi, \boldsymbol{b}^\phi\right) \textit{ represents a L.B. obtained by solving} \\ \textit{the dual of BLP - SSP}'_l, \forall(\boldsymbol{z}, \boldsymbol{b}), \textit{ except at current solution,} \left(\boldsymbol{z}^\phi, \boldsymbol{b}^\phi\right), \\ \textit{and } g(BLPSSP_l) \textit{ is the integer solution value at} \left(\boldsymbol{z}^\phi, \boldsymbol{b}^\phi\right) \end{array}\right) \\
&= \sum_{k\in J_l}\sum_{t\in T_l}(\theta_{kt} + \iota_{kt})z_{kt} + \sum_{j\in J_l}\sum_{t\in T_l}\lambda_{jt}z_{jt} + \sum_{t\in T_l}\left(\sum_{j\in J_l}\mu_{jt}\right)\left(\sum_{k\in J_l}z_{kt}\right) \\
&\quad - \sum_{j\in J_l}\sum_{t\in T_l}\left(\lambda_{jt} + \mu_{jt}\right)z_{0t} + |J_l|\sum_{j\in J_l}\sum_{k\in J_l, k\neq j}\sum_{t\in T_l}\kappa_{jkt}\left(b_{jt} + b_{kt}\right) - \sum_{j\in J_l}\sum_{t\in T_l}\lambda_{jt}b_{jt} \\
&\quad \underbrace{+ (|J_l| - 1)\sum_{j\in J_l}\sum_{k\in J_l, k\neq j}\sum_{t\in T_l}\kappa_{jkt} + \sum_{j\in J_l}\sum_{t\in T_l}\lambda_{jt}}_{c1^{sp}_{l\phi}} \\
&\quad + \left(g(\text{BLP - SSP}_l) - g\left(\text{BLP - SSP}'_l\right)\right) r^{sp}_{l\phi} \qquad \leftarrow \nu_{l\phi}
\end{aligned} \tag{2.41}$$

$$p^{sp}_{l\phi} = \left(\sum_{\substack{j\in J_l\cup\{0\} \\ t\in T_l \\ (j,t)\in \overline{Z}^{sp}_{l,1}}} z_{jt} + \sum_{\substack{j\in J_l \\ t\in T_l \\ (j,t)\in \overline{B}_{l,1}}} b_{jt}\right) - \left(\sum_{\substack{j\in J_l\cup\{0\} \\ t\in T_l \\ (j,t)\in \overline{Z}^{sp}_{l,0}}} z_{jt} + \sum_{\substack{j\in J_l \\ t\in T_l \\ (j,t)\in \overline{B}_{l,0}}} b_{jt}\right) \tag{2.42}$$

$$p^{sp}_{l\phi} \leq r^{sp}_{l\phi} + \underbrace{\left(\left|\overline{Z}^{sp}_{l,1}\right| + \left|\overline{B}_{l,1}\right| - 1\right)}_{c2^{sp}_{l\phi}} \qquad \leftarrow \xi_{l\phi} \tag{2.43}$$

$$p_{l\phi}^{sp} \geq \underbrace{\left(\left|\overline{Z}_{l,1}^{sp}\right| + \left|\overline{B}_{l,1}\right| - M_{l\phi}^{sp}\right)}_{c3_{l\phi}^{sp}} + M_{l\phi}^{sp} r_{l\phi}^{sp} \qquad \leftarrow \pi_{l\phi} \tag{2.44}$$

$$r_{l\phi}^{sp} \geq 0 \tag{2.45}$$

$$r_{l\phi}^{sp} \leq 1 \qquad \leftarrow \rho_{l\phi} \tag{2.46}$$

$$r_{l\phi}^{sp} \in \{0, 1\} \tag{2.47}$$

Proposition 1(a). *Constraints (2.41)—(2.47) are 'valid' optimality cuts to Model BLP-SP$_l$and therefore, lead to convergence between the solutions of Models BLP-SP$_l$and BLP-SSP$_l$.* **1(b).** *Constraints (2.41)—(2.47) offer a 'tighter' lower bound than the cuts proposed in Laporte and Louveaux* [48].

Proof of (1a). For all (**z**, **b**), the expression $\text{SSPC}_l \geq F\left(z, \boldsymbol{b} \middle| z^{\phi}, \boldsymbol{b}^{\phi}\right)$ represents the standard Benders optimality cut which is obtained by solving the dual of Model BLP - SSP$'_l$, i.e., the dual of relaxed Model BLP-SSP$_l$, and thus it is a valid optimality cut. Also, g(BLP-SSP$_l$) is the exact integer solution value corresponding to BLP-SSP$_l$, which is a valid lower bound on SSPC$_l$, but only for the current solution, $\left(z^{\phi}, \boldsymbol{b}^{\phi}\right)$.

Next, we show that the cut given by Eq. (3.41) reduces to, $\text{SSPC}_l \geq g(\text{BLP - SSP}_l)$, at the current solution, $\left(z^{\phi}, \boldsymbol{b}^{\phi}\right)$, corresponding to the ϕ^{th} iteration, and $\text{SSPC}_l \geq F\left(z, \boldsymbol{b} \middle| z^{\phi}, \boldsymbol{b}^{\phi}\right)$, for all $\{(z, \boldsymbol{b})\} \backslash \left(z^{\phi}, \boldsymbol{b}^{\phi}\right)$. Note that, at the current solution, $\left(z^{\phi}, \boldsymbol{b}^{\phi}\right)$, $F\left(z, \boldsymbol{b} \middle| z^{\phi}, \boldsymbol{b}^{\phi}\right) = F\left(z^{\phi}, \boldsymbol{b}^{\phi}\right) = g\left(\text{BLP - SSP}'_l\right)$, therefore, $g(\text{BLP - SSP}_l)$ can be rewritten as, $g(\text{BLP - SSP}_l) = F\left(z^{\phi}, \boldsymbol{b}^{\phi}\right) + \left(g(\text{BLP - SSP}_l) - g\left(\text{BLP - SSP}'_l\right)\right)$. Now, we only need to show that $r_{l\phi}^{sp}$ takes a value of 1 for $(z, \boldsymbol{b}) = \left(z^{\phi}, \boldsymbol{b}^{\phi}\right)$, and 0, for all $(z, \boldsymbol{b})$, except for $\left(z^{\phi}, \boldsymbol{b}^{\phi}\right)$, in order to prove the validity of the proposed cut. This is accomplished by enforcing the additional Constraints (2.42)—(2.47). Here, $\left|\overline{Z}_{l,1}^{sp}\right|$ and $\left|\overline{Z}_{l,0}^{sp}\right|$ represent indices of the z_{jt} variables that are equal to one and zero, respectively, in the current solution to BLP-SP$_l$. Similarly, $\overline{B}_{l,1}$ and $\overline{B}_{l,0}$ represent indices of the b_{jt} variables that are equal to one and zero, respectively, in the current solution of BLP-SP$_l$. An appropriate value for scalar, $M_{l\phi}^{sp}$, is $\left|\overline{Z}_{l,1}^{sp}\right| + \left|\overline{B}_{l,1}\right| + \left|\overline{Z}_{l,0}^{sp}\right| + \left|\overline{B}_{l,0}\right|$. Note that, $r_{l\phi}^{sp}$ takes a value of 1 if and only if a solution corresponding to Model BLP-SP$_l$ i.e., the values of variables that are input to Model BLP-SSP$_l$, i.e., $(z, \boldsymbol{b})$, repeat. However, this is not possible, since the number of solution pairs, $(z, \boldsymbol{b})$ is finite due to the binary nature of the variables. Therefore, the application of the proposed cuts is guaranteed to lead to convergence between solution values of Models BLP-SP$_l$ and BLP-SSP$_l$.

Proof of (1b).

To show the tightness of our cuts, we will now draw a comparison between cut (2.40) and cut (2.41) that we propose, (i.e., the optimality cut from BLP-SSP$_l$ to BLP-SP$_l$; note that the comparison to cut (2.51) will follow similarly). For ease of comprehension, we use the notation $\boldsymbol{x}$ to represent our variables $(z, \boldsymbol{b})$. We rewrite the optimality cut (2.41) for the ϕ^{th} iteration as follows (Note that w.l.o.g. we have suppressed subscript l):

$$SSPC_l \geq \begin{cases} g_{\boldsymbol{x}^{\phi}}(\text{BLP - SSP}) & \text{at } \boldsymbol{x} = \boldsymbol{x}^{\phi}, \\ g_{\boldsymbol{x}}\left(BLP - SSP'\right) \ \forall \boldsymbol{x} \in N_{\phi}(s) \subset \boldsymbol{X}, \ s \geq 1. \end{cases} \tag{2.48}$$

In combination with all the cuts added from iterations $k = 1, \ldots, \phi$, the above takes the following form:

$$SSPC_l \geq \begin{cases} \max\left\{g_{\boldsymbol{x}^\phi}(\text{BLP - SSP}), \underset{k=1,\ldots,\phi-1}{max}\left\{F\left(\boldsymbol{x}^\phi\middle|\boldsymbol{x}^k\right)\right\}\right\} = g_{\boldsymbol{x}^\phi}(\text{BLP - SSP}) \text{ at } \boldsymbol{x} = \boldsymbol{x}^\phi \\ \underset{k=1,\ldots,\phi-1}{max}\left\{F\left(\boldsymbol{x}\middle|\boldsymbol{x}^k\right) + \delta^+ \cdot r_\phi^{sp}\right\} \geq \text{LB}_\phi(s) \qquad \forall \boldsymbol{x} \in N_\phi(s) \subset \boldsymbol{X},\ s \geq 1, \end{cases} \tag{2.49}$$

where $\text{LB}_\phi(s)$ is obtained in a similar manner as $\lambda_r(s)$ in Equation.
(2.39) as follows:

$$\text{LB}_\phi(s) = \min\left\{\lambda\middle|\lambda \geq F\left(\boldsymbol{x}\middle|\boldsymbol{x}^k\right), \forall k = 1, \ldots, \phi\right\} \tag{2.50}$$

Since $F\left(\boldsymbol{x}\middle|\boldsymbol{x}^k\right)$ gives the value of continuous relaxation solution to the third stage (obtained using dual-based Benders cut corresponding to $\boldsymbol{x}^k$ solution of the second stage at some iteration, $k \leq \phi$), it is similar to using $R(\boldsymbol{x}) = R\left(\boldsymbol{x}^k\right) + \partial R\left(\boldsymbol{x}^k\right)\left(\boldsymbol{x} - \boldsymbol{x}^k\right)$ in the work of Laporte and Louveaux [48], and therefore, $\text{LB}_\phi(s) = \lambda_r(s) \geq L$, for all $s \geq 1$. Therefore, considering cut (2.49) for different values of s, we can see that, the lower bound on $SSPC_l$ (given by the right-hand side of the cut) has the same exact value as that of the lower bound on θ in Cut (2.40), for $s = 0, 1$, whereas, it is larger for $s \geq 2$.

Therefore, apart from the fact that we have developed a multi-cut version of optimality cuts compared to the single integer cut version proposed by Laporte and Louveaux [48], we have shown that our cuts offer a tighter lower bound on the value of an integer sub-problem in the context of Benders decomposition scheme. □

Remark Note that, Model BLP-SSP$_l$ will always be feasible for any given solution to Model BLP-SP$_l$. Therefore, we do not require the use of the feasibility cuts.

Optimality cut from BLP-SP$_l$to BLP-MP: For a given solution to Models BLP-MP and BLP-SP$_l$, if the MP-SP optimality gap is not within the optimality tolerance,τ^{mp}, we add the following set of optimality cuts (at iteration χ) to Model BLP-MP (Note that, the dual solution is obtained by solving Model BLP - SP$_l$′).

$$\begin{aligned} SPC_l &\geq \text{LB}_\chi \\ &= F\left(z, \boldsymbol{y}\middle|z^\chi, \boldsymbol{y}^\chi\right) + (g(\text{BLP - SP}_l) - g(\text{BLP - SP}_{l'}))r_{l\chi}^{mp} \\ &\left(\begin{array}{c} where F\left(z, \boldsymbol{y}\middle|z^\chi, \boldsymbol{y}^\chi\right) represents\ a\ L.B.\ obtained\ by\ solving\ the \\ dual\ of\ BFLPSP_{l'}, \forall(z, \boldsymbol{y}),\ except\ at\ current\ solution,\ \left(z^\chi, \boldsymbol{y}^\chi\right) \\ and\ g(BFLPSP_l) is\ the\ integer\ solution\ value\ at\left(z^\chi, \boldsymbol{y}^\chi\right). \end{array}\right) \\ &= \sum_{j\in J_l}\alpha_j z_j + \sum_{j\in J_l}\sum_{i\in NI_j}\gamma_{ij}y_{ij} + \beta_l s_l + E_{[\max]}\sum_{t\in T_l}\delta_t + \sum_{j\in J_l}\sum_{t\in T_l}\varepsilon_{jt} + \max_{j\in J_l}\{j\}\sum_{j\in J_l}\sum_{t\in T_l}\zeta_{jt} \\ &\quad + \sum_{t\in T_l}\eta_t + \sum_{\phi=1}^{\left|O_l^{SP}\right|}\left(c1_{l\phi}^{sp}\nu_{l\phi} + c2_{l\phi}^{sp}\xi_{l\phi} + c3_{l\phi}^{sp}\pi_{l\phi} + \rho_{l\phi}\right) + \left(g(\text{BLP - SP}_l) - g\left(\text{BLP - SP}_l'\right)\right)r_{l\chi}^{mp} \end{aligned} \tag{2.51}$$

$$p_{l\chi}^{mp} = \left(\sum_{\substack{j \in J_l \\ (j,\, t) \in \overline{Z}_{l,1}^{mp}}} z_j + \sum_{\substack{j \in J_l \\ i \in NI_j \\ (i,\, j) \in \overline{Y}_{l,1}}} y_{ij} \right) - \left(\sum_{\substack{j \in J_l \\ j \in \overline{Z}_{l,0}^{mp}}} z_j + \sum_{\substack{j \in J_l \\ i \in NI_j \\ (i,\, j) \in \overline{Y}_{l,0}}} y_{ij} \right) \tag{2.52}$$

$$p_{l\chi}^{mp} \leq r_{l\chi}^{mp} + \left(\left| \overline{Z}_{l,1}^{mp} \right| + \left| \overline{Y}_{l,1} \right| - 1 \right) \tag{2.53}$$

$$p_{l\chi}^{mp} \geq \left(\left| \overline{Z}_{l,1}^{mp} \right| + \left| \overline{Y}_{l,1} \right| \right) - M_{l\chi}^{mp} \left(1 - r_{l\chi}^{mp} \right) \tag{2.54}$$

$$r_{l\chi}^{mp} \in \{0,\, 1\} \tag{2.55}$$

Proposition 2(a) Constraints 2.51–2.55 are 'valid' optimality cuts to Model BLP-MP and therefore, lead to convergence between solutions of Models BLP-MP and BLP-SP$_l$. ***2(b).***Constraints 2.51—2.55 offer a 'tighter' lower bound than the cuts proposed in Laporte and Louveaux *[48]*.

The proof of this proposition follows along the same lines as that for Proposition 1(a) and 1(b), and it is omitted here for the sake of brevity (please see Singh [78] for details).

Remark Note that, Model BLP-SP$_l$ will always be feasible for any given solution to Model BLP-MP. Therefore, we do not require the use of feasibility cuts.

5 Results of computational investigation

In this section, we present computational results on the use of our proposed nested Benders decomposition method. We first discuss the results of our method for the cases of single and multiple BePs. We use the available GIS data for the catchment area of 48 km around Gretna, VA to perform the computational experiments. To put the effectiveness of the proposed nested Benders decomposition method in perspective, we then conduct experiments on a set of problem instances with different problem sizes using the state-of-the-art CPLEX® Branch-and-Bound method and CPLEX® Benders Strategy. Lastly, we compare the results of these methods with our proposed nested Benders decomposition method and demonstrate its effectiveness and superiority.

We refer to the use of the nested Benders decomposition method for Model BLP as Model BLP + NBD in our results, and it was tested by varying parameters such as switchgrass land use scenarios, and the use of various equipment systems (rear-loading rack, side-loading rack, and densification) pertinent to biomass logistics. Modeling for the constituent parts, namely, BLP-MP, BLP-SP$_l$, and BLP-SSP$_l$, and the associated workflow was accomplished using C + + Concert technology API of CPLEX® (12.6). CPLEX® was run in 'deterministic' mode with a maximum of 32 threads in parallel. All numerical tests were executed on Intel® Xeon® Processor E5-2687W, using 8 GB DDR3 memory. An optimality gap of 0.1% was set as the stopping criterion along with a time limit of 6,000 s of CPU run-time.

5.1 BLP + NBD for the case of a single BeP

We first considered the case of a single BeP located at the center of Gretna, VA, i.e.,$|L| = 1$. As a result, we did not include the transportation cost incurred from the BeP to the refinery. Comparisons are made for six production scenarios, which specify the land used for switchgrass production from the total available land area within 48 km around Gretna, VA, and they are 47,001 ha (Scenario 1), 49,747 ha (Scenario 2), 52,479 ha (Scenario 3), 57,151 (Scenario 4), 61,839 ha (Scenario 5), and 76,686 ha (Scenario 6) with the minimum amount of biomass required, BeP_{min}, fixed at 42,752 ha, 45,176 ha, 47,601 ha, 51,700 ha, 55,799 ha, and 68,847 ha, respectively, for the scenarios. This amounts to utilizing roughly 90% of the available biomass from the region for all the scenarios considered. We used a total of 1,000 production fields (i.e., $|I| = 1,000$) with all of them also serving as candidates for potential SSL locations for a region (i.e., $|J| = 1,000$), which constitutes a large-sized problem instance.

The cost of hauling a unit Mg (megagram = 1,000 kg = 1 metric tonne) of biomass from Field i to SSL j, f_{ij}, is obtained as follows [26]:

$$f_{ij} = f_i + f_2 d_{ij} = 3.3538 + 0.5856 d_{ij},$$

where f_1 and f_2 are fixed and variable cost parameters for in-field hauling, respectively, and d_{ij} is the travel distance between Field i and SSL j in km. The cost incurred for using the rack systems and the densification system for hauling a unit Mg of biomass on trucks from SSL_j to BeP_l (with their hauling capacity of 14.4 Mg/haul and 22.7 Mg/haul, respectively) is calculated as follows:

$$\begin{aligned} \mathrm{f_{jl}} &= \mathrm{f_2} + \mathrm{f_3 d_{jl}} \\ &= \begin{cases} 1.607 + 0.1381\mathrm{d_{jl}}, & rack\ system \\ 1.1747 + 0.0974\mathrm{d_{jl}}, & densification\ system \end{cases} \end{aligned}$$

where f_2 and f_3 are fixed and variable cost parameters respectively, for highway hauling with trucks, and d_{jl} is the travel distance between SSL_j and BeP_l in km. Thus, the total cost parameter for transporting biomass from Field i to BeP_l through SSL_j, f_{ijl} is given by

$$\mathrm{f_{ijl}} = \mathrm{f_{ij}} + \mathrm{f_{jl}}$$

The transportation cost for moving an equipment system from SSL_j to SSL_k, c_{jk}, is considered to be = \$2.29/km. Assuming the SSL loading operation is to be done using either of the two rack systems at 70% efficiency, the minimum and maximum SSL size is calculated assuming 3 days and 30 days of operation, respectively, amounting to $s_{[\min]} = 40.18ha$ and $s_{[\max]} = 401.79ha$ (= 21.6Mg/h × 10 h/day × 70% / 11.20 Mg/ha), respectively, where a rack system has an operational capacity of 21.6 Mg/ha and the average yield of switchgrass in the Gretna region is 11.2 Mg/ha. The equipment cost ($\mathrm{e_0}$) is assumed to be \$247,658.20 for the Rear-loading Rack system, \$142,471.70 for Side-loading Rack System, and \$769,227.0 for Densification System. The annual land rental fee, rc, used is = \$0.36/Mg [61].

We fixed a minimum amount required at each chosen BeP, $BeP_{[\min]}$, to ensure that the BeP operates at a certain economy of scale. $BeP_{[\min]}$ is fixed at 42,752, 45,172, 47,601, 51,700, 55,799, and 68,847 ha for the six scenarios, respectively. We assume that a fixed setup take-down cost, sc of \$600 is incurred to prepare an SSL for an equipment system. Further details of the data used in our experimentation can be found in Singh [78] and Resop et al. [64].

We now present the results of our experimentation in Table 4. Column 1 enumerates the

Table 4 Experimental results for 48 km around Gretna region using model BLP + NBD

Item	Scenario	CPU run-time (sec)	Total cost ($ m)	$/Mg	Number of			Avg. dist. (km)	
					Prod. Fields	SSLs	Equip. sets	Field to SSL	SSL to BeP
Comparison of equipment systems; Optimal solutions for									
Rear-loading Rack		2,920.00	11.50	24.01	806	358	12	0.804	42.170
Side-loading Rack	1	3,081.00	10.23	21.37	807	357	12	0.807	42.151
Densification		3,817.00	13.44	28.07	790	359	11	0.744	42.414
Optimal solutions for Side-loading Rack System	1	3,081.00	10.23	21.37	807	357	12	0.807	42.151
	2	4,054.00	11.37	22.48	840	372	12	0.819	41.770
	3	3,130.00	11.82	22.17	836	385	13	0.815	41.412
	4	3,458.00	12.49	21.57	846	407	14	0.819	40.972
	5	3,956.00	13.15	21.04	854	440	15	0.766	40.610
	6	5,675.00	16.38	21.25	941	542	19	0.660	41.356

types of equipment systems used in the experimentation. For each of the scenarios considered, program CPU run-time in secs, the total cost in $ (i.e., the objective function value of Model BLP + NBD, together with the additional cost of densification that is necessary at the BeP for the two rack systems), and the cost of production for a unit Mg of biomass utilized at the BeP are depicted in Columns 3, 4, and 5, respectively. Columns 6, 7, and 8 contains the number of production fields, SSLs, and equipment sets used, respectively, in the final solution at convergence within the set optimality criterion. Columns 9 and 10 display the average distance in km from a field to its associated SSL and from an SSL to its BeP, respectively. For l^{th} BeP (currently, we have, $l = 1$), the average distance from the fields to SSL is calculated as follows:

$$\frac{\sum_{j\in J_l}\sum_{i\in NI_j} d_{ij} ha_i y_{ij}}{\sum_{j\in J_l}\sum_{i\in NI_j} ha_i y_{ij}}$$

The average distance from the SSLs to the BeP is calculated as follows:

$$\frac{\sum_{j\in J_l} d_{jl}\left(\sum_{i\in NI_j} ha_i y_{ij}\right)}{\sum_{j\in J_l}\sum_{i\in NI_j} ha_i y_{ij}}$$

We now describe the results of Model BLP + NBD for the three different equipment systems, namely, 'rear-loading', 'side-loading' and, 'densification' (in which the biomass is densified at each SSL by using a densification system stationed at each SSL) under optimal setting, i.e., using all 1,000 potential SSL locations. We present the results in the first three rows of Table 4.

The 'side-loading' rack system performs the best among all three loading/unloading systems in terms of the total cost. Even though the 'densification' system can reduce the average distance of travel from a field to an SSL, its use cannot be justified because of the overall largest cost (resulting from the use of additional equipment). Since the objective value for the 'side-loading' rack system is the best among all three equipment systems, the remaining experiments were conducted with this equipment system only. These results are presented in the remaining Table 4, namely, the last six rows of the table, which depict the optimal solutions obtained for the scenarios by model BLP-NBD using the 'side-loading' rack system. The CPU run-times to obtain an optimal solution with the proposed method ranged from 2,920 s to 5,675 s with an average time of 3685.78 s across all the considered scenarios.

The average distance from the SSLs to BeP decreased continuously from Scenario 1 to Scenario 5 from 42.2 to 40.6 km and increased slightly to 41.4 km for Scenario 6. It reflects the location of various field types in the Gretna region. In particular, most of the cropland and pastureland are located close to the center while the scrubland and grasslands are concentrated on the outskirt.

5.1.1 BLP + NBD for the case of Multiple BePs

We now consider the biomass logistics problem in its entirety as stated earlier, i.e., we have two potential BeP locations, the first one at Bedford, VA, and the second at Gretna, VA. Note that, we now include the transportation costs incurred from BePs to the refinery as well. We consider the most conservative scenario for this analysis, i.e., Scenario 1, and evaluate the trend in the results for Model BLP + NBD by varying the amount of biomass required, i.e., the overall demand at the refinery, R. It is assumed that if a BeP is functional at either of these two locations, it will be operated at the minimum operational capacity of 478,822.40

Mg (= 42,752 ha × 11.2 Mg/ha). The maximum amount of biomass processed at either of the locations is based on the scenario availability, which is 526,411.20 Mg (= 47,001 ha × 11.2 Mg/ha) for Scenario 1 considered here.

Table 5 shows experimental results for various overall demands at the refinery from five different regions. Column 1 and 9 describe the availability of biomass in a region R (in Mg). Columns 2, 3, 4, 10, 11, 12, 13, and 14 represent the same entities as described earlier for Table 1. Column 5, 6, 7, and 8 display the railway transportation cost between BeP and refinery, total BePs, average distance between a BeP and refinery (in km), and BeP number (1 or 2) respectively. The first two rows of the Table 5 contain results from regions with biomass yield (R) of 478,822.40 Mg and 526,411.20 Mg respectively. Understandably, two BePs are used for the values of R that exceed the maximum availability in one region, i.e., R = 957,644.80 Mg, 1,005,233.60 Mg, and 1,052,822.40 Mg. Thereby, the last six rows of the table show the results from these three regions. The unit cost of production increases from 44.69 $/Mg to 46.03 $/Mg as the biomass requirement at the refinery enforces the logistics system for a single BeP's region to utilize 100% of the available biomass, i.e., from R = 478,822.40 Mg to R = 526,411.20 Mg. A similar trend is observed even when two BePs are used. For R = 957,644.80 Mg, both the BePs only process the amount equal to their minimum capacity, i.e., 478,822.40 Mg. As R is increased to 1,052,822.40 Mg, both the BeP regions operate so as to utilize the maximum available biomass in their respective regions. For R = 1,005,233.60 Mg, the total demand at the refinery is between the minimum capacity of both BePs combined and the total available biomass from both regions. In view of the optimal solution, the amount that is processed by either of the BePs lies somewhere between their minimum and maximum processing capacities. For the first BeP that is closer to the refinery, it is 511,660.80 Mg, which is more than 493,572.80 Mg for the second BeP. The average distance (in km) from BeP to refinery ranges from 297 to 330.5 with an overall average distance to the refinery of 321.974 km. The total cost ($ in millions) of production for the regions range from 20.14 to 50.13. This includes the rail transportation cost ($ in millions) given in column 5 of Table 5. The average CPU run-time of the model over these test cases is 3,330.00 secs, whereas the maximum run-time is 4,904.00 secs.

For the conservative yield scenario that was considered, i.e., Scenario 1, the maximum amount of ethanol that can be produced is 78.1 million gallons (MG) by using the two BePs at Gretna, VA, and Bedford, VA. The incurred a total cost of $50.13 million which amounts to a unit cost of production at $0.64/gallon. Note that the cost of conversion from bio-crude to ethanol at the refinery is not included in this analysis. The effectiveness of the results obtained by varying land use for biomass production and demand at the refinery demonstrates the applicability of the methodology developed to real-life scenarios.

5.2 Experiments using the state-of-the-art Branch-and-Bound and Benders Strategy algorithms of CPLEX® solver for the solution of Model BLP

As alluded to earlier, we use CPLEX® Branch-and-Bound method (denoted as BLP + BB) and CPLEX® Benders Strategy (denoted as BLP + BS) to directly solve Model BLP. While running all experiments both primal and dual reductions were allowed during the pre-reduction parameter selection i.e., the CPLEX® solver's reduce parameter is set to option 3. It is observed that this option led to faster convergence and lower computation times in comparison with options that restricted the CPLEX® solver to either only primal reductions or only dual reductions. In addition, the CPLEX® Benders Strategy parameter is set to full for all the BLP + BS experiments. This parameter gives full autonomy to the CPLEX® solver

Table 5 Experimental results for overall demand at refinery with two potential BeP regions—Gretna, VA and Bedford, VA using model BLP + NBD

Biomass R (Mg)	CPU run-time (secs)	Total cost ($ in millions)	$/Mg	Rail cost ($ in millions)	BePs used	Avg. dist. (km) BeP to refinery	BeP	Biomass R(Mg)	Number of			Average distance (km)	
									Prod. fields	SSLs	Equip. sets	Field to SSL	SSL to BeP
478,822.40	3,081.00	21.40	44.69	11.17	1	297.000	1	478,822.40	807	357	12	0.807	42.151
526,411.20	2,601.00	24.23	46.03	12.28	1	297.000	1	526,411.20	962	398	13	0.928	43.617
957,644.80	3,215.00	44.31	46.27	23.84	2	330.500	1	478,822.40	807	357	12	0.807	42.151
							2	478,822.40	807	357	12	0.807	42.151
1,005,233.60	4,904.00	50.00	47.75	25.00	2	329.897	1	511,660.80	895	385	13	0.856	43.200
							2	493,572.80	844	368	12	0.833	42.612
1,052,822.40	2,848.00	50.13	47.61	26.21	2	330.500	1	526,411.20	962	398	13	0.928	43.617
							2	526,411.20	962	398	13	0.928	43.617

Table 6 Experimental results from direct solution of Model BLP using CPLEX® algorithms

PROBLEM INSTANCES			BLP + BB	BLP + BS
Prod. Fields	Number of SSLs	BeP	MIP Optimality gap (CPU run- time (seconds))	MIP Optimality gap (CPU run-time (seconds))
10	6	3	0.00% (0.23)	0.32% (1.14)
100	20	1	5.85%	7.50%
100	50	1	7.27%	7.83%
150	20	1	2.62%	5.82%
150	50	1	8.78%	11.39%
150	75	1	7.78%	44.49%
200	80	1	9.36%	35.05%
200	100	1	11.18%	50.55%
250	100	1	6.91%	38.36%
250	150	1	10.66%	46.21%
500	200	1	12.53%	40.62%
500	300	1	10.59%	43.35%
1000	400	1	15.70%	82.63%
1000	600	1	20.94%	82.79%

to decompose the problem without any manual input or intervention. An optimality gap of 0.1% was set as the stopping criterion along with an increased time limit of 10,000 s of CPU run-time. To study the convergence behaviors of these methods, the problem instances were constructed by varying the number of fields, SSLs, and BEPs. The location coordinates of the Fields for all the instances were generated randomly from a uniform distribution. All other data inputs like the constants, boundary conditions, etc. were chosen as necessary to ensure that the problem stays feasible.

First, we make remarks on the convergence behaviors observed for BLP + BB and BLP + BS. Table 6 shows the results from direct solution of Model BLP using CPLEX® algorithms. The first column enumerates the 'Problem Instances' with each instance representing 'Number of Production Fields, SSLs, and BePs'. The second and third columns in Table 6 represent 'MIP Optimality Gaps' for CPLEX® BLP + BB and BLP + BS algorithms respectively. In general, it is observed that the MIP optimality gaps for both the direct CPLEX® methods increased with the increment in problem size. This trend is also observed in the convergence rate vs CPU run-time. For all instances, a faster convergence was observed initially to a certain MIP gap followed by a very slow nominal improvement in their values. The BLP + BB achieved MIP optimality gaps ranging from 13.67% to 23.86% in 212.19 to 5423.31 s of CPU run-time. BLP + BS on the other hand converged relatively slower, with most runs converging to MIP optimality gaps of 35.94% to 82.79% in CPU run-times ranging from 403.53 to 3147.56 s. As the problem size increased the overall convergence got slower and slower for both BLP + BB and BLP + BS. Note that, BLP + BB outperforms BLP + BS as the MIP optimality gaps are consistently higher for BLP + BS for all the problem instances.

Regarding comparative performances of BLP + NBD, BLP + BB, and BLP + BS: Both BLP + BB and BLP + BS are not able to solve 13 out of 14 problem instances to optimality

within the allowed time limit. Moreover, both BLP + BB and BLP + BS encountered memory issues during computation experiments for the problem instances of size 1,000 fields, and 400/600 SSLs. Furthermore, the fact that BLP + BB (a better performer between BLP + BB and BLP + BS) is only able to get to a 5.85% MIP optimality gap for a problem instance of size as small as 100 fields and 20 SSLs itself demonstrates the difficulty of solving the BLP by these methods. Even on the higher side of the problem instance size spectrum (i.e., problem instance of size 1000 fields and 400 SSLs), BLP + BB can only get to a 15.70% MIP optimality gap. The experimental results in Tables 4 and 5 demonstrate the effectiveness and ability of BLP + NBD to solve real-life-sized problem instances (of scale: 800–1000 Production Fields and 350–400 SSLs) to optimality in 2,848 to 5,675 s of CPU run-time. It clearly illustrates the superiority of the proposed BLP + NBD algorithm over BLP + BB and BLP + BS. This result was expected as the optimality cuts developed in Sect. 4.1 were shown to be superior to those given in the literature and lead to faster convergence.

6 Concluding remarks

In this paper, we have presented a biomass logistics system for the production of ethanol from seasonal switchgrass in the Upper Southeast region of the US. We have considered features of locating SSLs and allocating production fields to SSLs and the SSLs to the BePs. We have also explicitly included routing of loading/unloading/ processing equipment sets among the SSLs to help process biomass at the SSLs. This feature complicates the problem. We developed a mathematical model to capture all of these features. We solved this model by decomposing it into three smaller problems based on the Nested Benders decomposition scheme. The novelty of the proposed decomposition scheme is that the sub-problems are solved as integer programs rather than as their LP relaxations. We proposed a multi-cut version of Laporte and Louveaux's [48] based optimality cuts that can capture solution value at an integer solution for the sub-problem(s). We have shown the validity, tightness, and feasibility of these cuts and that they lead to the convergence of our proposed decomposition scheme. We also show these cuts to be stronger than those proposed by Laporte and Louveaux [48]. Furthermore, we have demonstrated the applicability of our proposed approach to real-life-sized problem instances. In addition, we observe that the proposed algorithm outperforms the CPLEX® based algorithms.

We first considered a single bio-energy plant (BeP) operation under a single harvest scenario and drew comparisons among three different types of equipment systems used for handling biomass at an SSL. The 'side-loading' rack system is found to give the smallest total cost. Consequently, we use this system in all the remaining test cases studied. The optimal solution corresponding to the use of this equipment system is obtained in 3,081.00 secs, having a total cost of $10.23M and a unit cost of $21.37/Mg. The maximum average field to SSL distance is obtained to be 0.819 km, and the maximum average distance from the SSLs to the BeP is obtained to be 42.151 km for our model. We have also presented results on the use of the proposed methodology in the case of multiple BePs, which includes the logistics operations for two BeP locations. We considered five BeP test region cases by varying the amount of total biomass intake required at the refinery, to study its impact on the solution obtained and, on the run-time, required. The average CPU run-time of the model over these test cases is 3,330.00 secs, whereas the maximum run-time is 4,904.00 secs. The maximum amount of ethanol that can be produced by using two BePs, one at Gretna, VA and the other at Bedford, VA is 78.1 million gallons (MG), incurring a total cost of $50.13M.

This amounts to a unit production cost for ethanol to be \$0.64/gallon. The effectiveness of the results obtained by varying land use for biomass production and demand at the refinery has demonstrated the applicability of the methodology developed to real-life scenarios.

Lastly, we observe that the state-of-the-art solver CPLEX® based methods were at best able to converge to a 5.85% MIP gap in 10,000 s for a problem instance of size as small as 100 fields and 20 SSLs. On the other hand, the proposed BLP + NBD can solve large-sized instances of the scale of 1,000 Fields and 1,000 potential SSLs to optimality in around 3,500 s of CPU run-time, thereby establishing the effectiveness of our proposed BLP + NBD algorithm.

For future work, we propose consideration of a stochastic environment in which biomass availability, demand at the refinery, and other parameters are affected by uncertainty.

Funding This research did not receive any specific grant from funding agencies in the public, commercial, or not-for-profit sectors.

Data availability The datasets used during the computational investigation in the Sects. 6.1.1 and 6.1.2 are from literature appropriately cited in the text. The datasets analysed during and/or generated in Sect. 6.2 are not publicly available as these correspond to randomly constructed problem instances but are available from the corresponding author on reasonable request.

Declarations

Competing interests The authors have no competing interests to declare that are relevant to the content of this article.

Informed Consent All authors certify that they have no affiliations with or involvement in any organization or entity with any financial interest or non-financial interest in the subject matter or materials discussed in this manuscript.

References

1. Aboytes-Ojeda, M., Castillo-Villar, K.K., and Eksioglu, S.D.: Modeling and optimization of biomass quality variability for decision support systems in biomass supply chains. Ann. Oper. Res. 1–28 (2019)
2. Ali, A., Arani, H.V., Dashti, H.: A stochastic programming approach towards optimization of biofuel supply chain. Energy **76**, 513–525 (2014)
3. Aguayo, M.M., Sarin, S.C., Cundiff, J.S.: A branch-and-price approach for a biomass feedstock logistics supply chain design problem. IISE Trans. **51**(12), 1348–1364 (2019)
4. Aguayo, M.M., Sarin, S.C., Cundiff, J.S., Comer, K., Clark, T.: A corn-stover harvest scheduling problem arising in cellulosic ethanol production. Biomass Bioenerg. **107**, 102–112 (2017)
5. Akgul, O., Zamboni, A., Bezzo, F., Shah, N., Papageorgiou, L.G.: Optimization-based approaches for bioethanol supply chains. Ind. Eng. Chem. Res. **50**(9), 4727–4938 (2010)
6. Akhtari, S., Sowlati, T., Griess, V.C.: Integrated strategic and tactical optimization of forest-based biomass supply chains to consider medium-term supply and demand variations. Appl. Energy **213**, 626–638 (2018)
7. An, H., Wilhelm, W.E., Searcy, S.W.: A mathematical model to design a lignocellulosic biofuel supply chain system with a case study based on a region in Central Texas. Bioresour. Technol. **102**, 7860–7870 (2011)

8. Angulo, G., Ahmed, S., and Dey, S.S.: Improving the integer L-shaped method. INFORMS J. Comput. 28(3), 483–499. https://doi.org/10.1287/ijoc.2016.0695 (2016)
9. Awudu, I., Zhang, J.: Uncertainties and sustainability concepts in biofuel supply chain management: a review. Renew. Sustain. Energy Rev. **16**, 1359–1368 (2012)
10. Azadeh, A., Irani, H.V., Dasti, H.: A stochastic program approach towards optimization of biofuel supply chain. Energy **76**, 513–525 (2014)
11. Babazadeh, R., Razmi, J., Pishvaee, M.S., and Rabbani, M.: A sustainable second-generation biodiesel supply chain network design problem under risk. Omega. **66** (Part B), 258–277 (2017a)
12. Bai, Y., Hwang, T., Kang, S., Ouyang, Y.: Biofuel refinery location and supply chain planning under traffic congestion. Transp. Res. Part B Methodol. **45**(1), 162–175 (2011)
13. Bai, Y., Li, X., Peng, F., Wang, X., Ouyang, Y.: Effects of disruption risks on biorefinery location design. Energies **8**(2), 1468–1486 (2015)
14. Bai, Y., Ouyang, Y., Pang, J.S.: Biofuel supply chain design under competitive agricultural land use and feedstock market equilibrium. Energy Econ. **34**, 1623–1633 (2012)
15. Bai, Y., Ouyang, Y., Pang, J.S.: Enhanced models and improved solution for competitive biofuel supply chain design under land use constraints. Eur. J. Oper. Res. **249**, 281–297 (2016)
16. Bairamzadeh, S., Pishvaee, M.S., Saidi-Mehrabad, M.: Multi-objective robust possibilistic programming approach to sustainable bioethanol supply chain design under multiple uncertainties. Ind. Eng. Chem. Res. **55**(1), 237–256 (2016)
17. Balaman, E.Y. and Hasan, S.: Sustainable design of renewable energy supply chains integrated with district heating systems: a fuzzy optimization approach. J. Clean. Prod. **133** (Supplement C), 863–885 (2016)
18. Benders, J.F.: Partitioning procedures for solving mixed-variables programming problems. Numer. Math. **4**(1), 238–252 (1962)
19. Birge, J.R.: Decomposition and partitioning methods for multistage stochastic linear programs. Oper. Res. **33**(5), 989–1007 (1985)
20. Bowling, I.M., Ponce-Ortega, J.M., El-Halwagi, M.M.: Facility location and supply chain optimization for a biorefinery. Ind. Eng. Chem. Res. **50**(10), 6276–6286 (2011)
21. Cambero, C., Sowlati, T., and Pavel, M.: Economic and life cycle environmental optimization of forest-based biorefinery supply chains for bioenergy and biofuel production. Chem. Eng. Res. Des. **107** (Supplement C), 218–235 (2016)
22. Castillo-Villar, K.K., Eksioglu, S., Taherkhorsandi, M.: Integrating biomass quality variability in stochastic supply chain modeling and optimization for large-scale biofuel production. J. Clean. Prod. **149**, 904–918 (2017)
23. Chen, C.W., Fan, Y.: Bioethanol supply chain system planning under supply and demand uncertainties. Transp. Res. Part E Logistics Transp. Rev. **48**(1), 150–164 (2012)
24. Chen, X. and Onal, H.: An economic analysis of the future U.S. biofuel industry, facility location, and supply chain Network. Transp. Sci. **48** (4), 575- 591 (2014)
25. Cucek, L., Varbanov, P.S., Klemes, J.J., Kravanja, Z.: Total footprints-based multi-criteria optimization of regional biomass energy supply chains. Energy **44**(1), 135–145 (2012)
26. Cundiff, J.S., Grisso, D., and Shapouri, H.: Economic analysis of two receiving facility designs for a boenergy plant. In: American Society of Agricultural and Biological Engineers (ASAE), Annual Meeting, page 1 (2007)
27. Cundiff, J.S., Dias, N., Sherali, H.: A linear programming approach for designing a herbaceous biomass delivery system. Biores. Technol. **59**(1), 47–55 (1997)
28. Dal-Mas, M., Giarola, S., Zamboni, A., Bezzo, F.: Strategic design and investment capacity planning of the ethanol supply chain under price uncertainty. Biomass Bioenerg. **35**(5), 2059–2071 (2011)
29. De Jong, S., Hoefnagels, R., Wetterlund, E., Pettersson, K., Faaij, A., Junginger, M.: Cost optimization of biofuel production-the impact of scale, integration, transport and supply chain configurations. Appl. Energy **195**, 1055–1070 (2017)
30. De Meyer, A., Cattrysse, D., Rasinmäki, J., Van Orshoven, J.: Methods to optimise the design and management of biomassfor-bioenergy supply chains: a review. Renew. Sustain. Energy Rev. **31**, 657–670 (2014)
31. De Mol, R.M., Jogens, M.A.H., van Beek, P., Gigler, J.K.: Simulation and optimization of the logistics of biomass fuel collection. Netherland J. Agric. Sci. **45**, 219–228 (1997)
32. Desrochers, M., Laporte, G.: Improvements and extensions to the miller-tucker-zemlin subtour elimination constraints. Oper. Res. Lett. **10**(1), 27–36 (1991)
33. Dunnett, A.J., Adjiman, C., Shah, N.: Biomass to heat supply chains: applications of process optimization. Process Saf. Environ. Prot. **85**(5), 419–429 (2007)

34. Dunnett, A.J., Adjiman, C., Shah, N.: A spatially explicit whole system model of the lignocellulosic bioethanol supply chain: an assessment of decentralised processing potential. Biotechnol. Biofuels **1**(1), 13 (2008)
35. Fales, S.L., Hess, J.R., Wilhelm, W., Erbach, D., Provine, W.D., Vogel, K.P., Peterson, T.A., and Runge, E.C.A.: Convergence of agriculture and energy: producing cellulosic biomass for biofuels. Publications from USDA-ARS/UNL Faculty, pp 291 (2007)
36. Frombo, F., Minciardi, R., Robba, M., Rosso, F., Sacile, R.: Planning woody biomass logistics for energy production: a strategic decision model. Biomass Bioenerg. **33**(3), 372–383 (2009)
37. Flisberg, P., Frisk, M., Ronnqvist, M.: FuelOpt: a decision support system for forest fuel logistics. J. Oper. Res. Soc. **63**(11), 1600–1612 (2012)
38. Gebreslassie, B.H., Yao, Y., You, F.: Design under uncertainty of hydrocarbon biorefinery supply chains: multiobjective stochastic programming models, decomposition algorithm, and a comparison between cvar and downside risk. AIChE J. **58**(7), 2155–2179 (2012)
39. Gilani, H., Sahebi, H., Oliveira, F.: Sustainable sugarcane-to-bioethanol supply chain network design: a robust possibilistic programming model. Appl. Energy **278**, 115653 (2020)
40. Gunnarsson, H., Ronnqvist, M., Lundgren, J.T.: Supply chain modelling of forest fuel. Eur. J. Oper. Res. **158**(1), 103–123 (2004)
41. Hu, H., Lin, T., Wang, S., Rodriguez, L.F.: A cyberGIS approach to uncertainty and sensitivity analysis in biomass supply chain optimization. Appl. Energy **203**, 26–40 (2017)
42. Huang, Y., Fan, Y., Chen, C.W.: An integrated biofuel supply chain to cope with feedstock seasonality and uncertainty. Transp. Sci. **48**(4), 540–554 (2014)
43. Judd, J.D., Sarin, S.C., Cundiff, J.S.: Design, modeling, and analysis of a feedstock logistics system. Biores. Technol. **103**(1), 209–218 (2012)
44. Kim, J., Realff, M.J., Lee, J.H.: Optimal design and global sensitivity analysis of biomass supply chain networks for biofuels under uncertainty. Comput. Chem. Eng. **35**(9), 1738–1751 (2011)
45. Lahyani, R., Coelho, L.C., Renaud, J.: Alternative formulations and improved bounds for the multi-depot fleet size and mix vehicle routing problem. OR Spect. **40**, 125–157 (2018)
46. Lamers, P., Roni, M.S., Tumuru, K.G., Jacobson, J.J., Cafferty, K.G., Hansen, J.K., Bals, B.: Techno-economic analysis of decentralized biomass processing depots. Biores. Technol. **194**, 205–213 (2015)
47. Lam, H.L., Klemes, J.J., Kravanja, Z.: Model-size reduction techniques for large-scale biomass production and supply networks. Energy **36**(8), 4599–4608 (2011)
48. Laporte, G., Louveaux, F.V.: The integer L-shaped method for stochastic integer programs with complete recourse. Oper. Res. Lett. **13**(3), 133–142 (1993)
49. Lin, T., Rodríguez, L.F., Shastri, Y.N., Hansen, A.C., Ting, K.: GIS enabled biomass-ethanol supply chain optimization: model development and Miscanthus application. Biofuels Bioprod. Biorefin. **7**, 314–333 (2013)
50. Liu, Z., Qiu, T., Chen, B.: A study of the LCA based biofuel supply chain multi-objective optimization model with multi-conversion paths in China. Appl. Energy **126**, 221–234 (2014)
51. Louveaux, F.V.: A solution method for multistage stochastic programs with recourse with application to an energy investment problem. Oper. Res. **28**(4), 889–902 (1980)
52. Mafakheri, F., Nasiri, F.: Modeling of biomass-to-energy supply chain operations: applications, challenges and research directions. Energy Policy **67**, 116–126 (2014)
53. Malladi, K.T., Sowlati, T.: Bi-objective optimization of biomass supply chains considering carbon pricing policies. Appl. Energy **264**, 114719 (2020)
54. Mapemba, L.D., Epplin, F.M., Huhnke, R.L., Taliaferro, C.M.: Herbaceous plant biomass harvest and delivery cost with harvest segmented by month and number of harvest machines endogenously determined. Biomass Bioenerg. **32**(11), 1016–1027 (2008)
55. Mapemba, L.D., Epplin, F.M., Taliaferro, C.M., Huhnke, R.L.: Biorefinery feedstock production on conservation reserve program land. Appl. Econ. Perspect. Policy **29**(2), 227–246 (2007)
56. Marufuzzaman, M., Sandra, D., Ioglu, E., Huang, Y.: Two-stage Stochastic programming supply chain model for biodiesel production via wastewater treatment. Comput. Oper. Res. **49**, 1–17 (2014)
57. Mavrotas, G.: Effective Implementation of the e-constraint method in multi objective mathematical programming problems. Appl. Math. Comput. **213**(2), 455–465 (2009)
58. Memişoğlu, G., Üster, H.: Design of a biofuel supply network under stochastic and price-dependent biomass availability. IISE Trans. **53**(8), 869–882 (2021)
59. Miller, C.E., Tucker, A.W., Zemlin, R.A.: Integer programming formulation of traveling salesman problems. J. ACM (JACM) **7**(4), 326–329 (1960)
60. Miret, C., Chazara, P., Montastruc, L., Negny, S., and Domenech, S.: Design of Bioethanol Green Supply Chain: a comparison between first and second generation biomass concerning economic, environmental and social criteria. Comput. Chem. Eng. **85** (Supplement C), 16–35 (2016)

61. Morey, R.V., Kaliyan, N., Tiffany, D.G., Schmidt, D.R.: A corn stover supply logistics system. Appl. Eng. Agric. **26**(3), 455–461 (2010)
62. Nur, F., Aboytes-Ojeda, M., Castillo-Villar, K.K., and Marufuzzaman, M.: A two-stage stochastic programming model for biofuel supply chain network design with biomass quality implications, IISE Trans. **53**:8, 845–868. https://doi.org/10.1080/24725854.2020.1751347 (2021)
63. Ortiz-Gutiérrez, R.A., Giarola, S., Bezzo, F.: Optimal design of ethanol supply chains considering carbon trading effects and multiple technologies for side-product exploitation. Environ. Technol. **34**, 2189–2199 (2013)
64. Pereira, M.V.F., Pinto, L.M.V.G.: Stochastic optimization of a multi-reservoir hydroelectric system: a decomposition approach. Water Resour. Res. **21**(6), 779–792 (1985)
65. Poudel, S.R., Marufuzzaman, M., Bian, L.: A hybrid decomposition algorithm for designing a multi-modal transportation network under biomass supply uncertainty. Transp. Res. Part E Log. Transp. Rev. **94**, 1–25 (2016)
66. Poudel, S.R., Quddus, M.A., Marufuzzaman, M., Bian, L., and Burch V, R.F.: Managing congestion in a multi-modal transportation network under biomass supply uncertainty. Ann. Oper. Res. **273**(1–2), 739–781 (2019)
67. Pourjavad, E., Shahin, A.: The application of Mamdani fuzzy inference system in evaluating green supply chain management performance. Int. J. Fuzzy Syst. **20**, 901–912 (2018)
68. Quddus, M.A., Chowdhury, S., Marufuzzaman, M., Yu, F., Bian, L.: A two-stage chance-constrained stochastic programming model for a bio-fuel supply chain network. Int. J. Prod. Econ. **195**, 27–44 (2018)
69. Ren, J., Dong, L., Sun, L., Goodsite, M.E., Tan, S., and Dong, L.: Life cycle cost optimization of biofuel supply chains under uncertainties based on interval linear programming. Bioresource Technol. **187** (Supplement C), 6–13 (2015)
70. Resop, J.P., Cundiff, J.S., Heatwole, C.D.: Spatial analysis to site satellite storage locations for herbaceous biomass in the piedmont of the southeast. Appl. Eng. Agric. **27**(1), 25–32 (2011)
71. Sarkar, B., Mridha, B., Pareek, S., Sarkar, M., Thangavelu, L.: A flexible biofuel and bioenergy production system with transportation disruption under a sustainable supply chain network. J. Clean. Prod. **317**, 128079 (2021)
72. Savoji, H., Mousavi, S.M., Antucheviciene, J., Pavlovskis, M.: A robust possibilistic bi-objective mixed integer model for green biofuel supply chain design under uncertain conditions. Sustainability **14**(20), 13675 (2022)
73. Shabani, N., Sowlati, T.: A mixed integer nonlinear programming model for tactical value chain optimization of a wood biomass power plant. Appl. Energy **104**, 353–361 (2013)
74. Shabani, N., Sowlati, T., Ouhimmou, M., Ronnqvist, M.: Tactical supply chain planning for a forest biomass power plant under supply uncertainty. Energy **78**, 346–355 (2014)
75. Shabani, N. and Sowlati, T.: A hybrid multi-stage stochastic programming robust optimization model for maximizing the supply chain of a forest-based biomass power plant considering uncertainties. J. Clean. Prod. **112** (Part 4), 3285–3293 (2016)
76. Sharma, B., Ingalls, R.G., Jones, C.L., Huhnke, R.L., Khanchi, A.: Scenario optimization modeling approach for design and management of biomass-to-biorefinery supply chain system. Biores. Technol. **150**, 163–171 (2013)
77. Shastri, Y., Hansen, A., Rodriguez, L., Ting, K.C.: Development and application of biofeed model for optimization of herbaceous biomass feedstock production. Biomass Bioenerg. **35**(7), 2961–2974 (2011)
78. Singh, S.: Modeling, analysis, and algorithmic development of some scheduling and logistics problems arising in biomass supply chain, hybrid flow shops, and assembly job shops. Dissertation, Grado Department of Industrial and Systems Engineering, Virginia Tech, Blacksburg, VA 24061. http://hdl.handle.net/10919/91466 (2019). Accessed June 2019
79. Sun, F., Aguayo, M.M., Ramachandran, R., Sarin, S.C.: Biomass feedstock supply chain design: a taxonomic review and a decomposition-based methodology. Int. J. Prod. Res. **56**(17), 5626–5659 (2018)
80. Sun, F., Sarin, S.C., Cundiff, J.S., Sert, I.O.: Design of cost-effective sorghum biomass feedstock logistics-a comparison of different systems. Biomass Bioenerg. **143**, 105823 (2020)
81. Sun, F., Sarin, S. C., and Kothyari, A.: Biomass feedstock logistics with mobile equipment. Informatica (accepted)
82. Üster, H., Memişoğlu, G.: Biomass logistics network design under price-based supply and yield uncertainty. Transp. Sci. **52**(2), 474–492 (2018)
83. Xie, F., Huang, Y., Eksioglu, S.: Integrating multimodal transport into cellulosic biofuel supply chain design under feedstock seasonality with a case study based on California. Bioresour. Technol. **152**, 15–23 (2014)

84. You, F., Tao, L., Graziano, D.J., Snyder, S.W.: Optimal design of sustainable cellulosic biofuel supply chains: multi-objective optimization coupled with life cycle assessment and input-output analysis. A/ChE J. **58**(4), 1157–1180 (2012)
85. Yue, D., Slivinsky, M., Sumpter, J., You, F.: Sustainable design and operation of cellulosic bioelectricity supply chain networks with life cycle economic, environmental, and social optimization. Ind. Eng. Chem. Res. **53**(10), 4008–4029 (2014)
86. Zamar, D.S., Gopaluni, B., Sokhansanj, S., Newlands, N.K.: A quantile-based scenario analysis approach to biomass supply chain optimization under uncertainty. Comput. Chem. Eng. **97**, 114–123 (2017)
87. Zamboni, A., Shah, N., and Bezzo, F.: Spatially explicit static model for the strategic design of future bioethanol production systems. 2. Multi-objective environmental optimization. Energy Fuels. **23**, 5134–5143 (2009)
88. Zarei, M., Niaz, H., Dickson, R., Ryu, J.H., Liu, J.J.: Optimal design of the biofuel supply chain utilizing multiple feedstocks: a Korean case study. ACS Sustain. Chem. Eng. **9**, 14690–14703 (2021)
89. Zarrinpoor, N., Khani, A.: Designing a sustainable biofuel supply chain by considering carbon policies: a case study in Iran. Energy Sustain. Soc. **11**, 38 (2021)
90. Zhang, J., Atif, O., Iddrisu, A., Gonela, V.: An integrated optimization model for switchgrass-based bioethanol supply chain. Appl. Energy **102**, 1205–1217 (2013)
91. Zhang, B., Guo, C., Lin, T., Faaij, A.P.C.: Economic optimization for a dual-feedstock lignocellulosic-based sustainable biofuel supply chain considering greenhouse gas emission and soil carbon stock. Biofuels Bioprod. Biorefining **16**, 653–670 (2022)
92. Zhang, B., Hastings, A., Clifton-Brown, J.C., Jiang, D. and Faaij, A.P.C.: Modeled spatial assessment of biomass productivity and technical potential of Miscanthus × giganteus, *Panicum virgatum* L., and Jatropha on marginal land in China. GCB Bioenergy. **12**, 328–345 (2020)
93. Zhu, X., Li, X., Yao, Q., Chen, Y.: Challenges and models in supporting logistics system design for dedicated-biomass-based bioenergy industry. Biores. Technol. **102**(2), 1344–1351 (2011)
94. Zuo, M., Kuo, W., McRoberts, K.L.: Application of mathematical programming to a large-scale agricultural production and distribution system. J. Oper. Res. Soc. **42**(8), 639–648 (1991)

Authors and Affiliations

Sanchit Singh[1] · Subhash C. Sarin[1] · Sandeep Singh Sangha[1]

✉ Sanchit Singh

Subhash C. Sarin
sarins@vt.edu

Sandeep Singh Sangha
sandeepsangha@vt.edu

[1] Virginia Polytechnic Institute and State University, Blacksburg, VA, USA